NATIONAL ADVISORY COMMITTEE FOR AERONAUTICS

REPORT No. 539

INVESTIGATION OF FULL-SCALE SPLIT TRAILING-EDGE WING FLAPS WITH VARIOUS CHORDS AND HINGE LOCATIONS

By RUDOLF WALLACE

1935

For sale by the Superintendent of Documents, Washington, D. C. - - - - - - - - - - - - - - Price 10 cents
Subscription price, $3 per year

AERONAUTIC SYMBOLS

1. FUNDAMENTAL AND DERIVED UNITS

	Symbol	Metric		English	
		Unit	Abbreviation	Unit	Abbreviation
Length	l	meter	m	foot (or mile)	ft. (or mi.)
Time	t	second	s	second (or hour)	sec. (or hr.)
Force	F	weight of 1 kilogram	kg	weight of 1 pound	lb.
Power	P	horsepower (metric)		horsepower	hp.
Speed	V	kilometers per hour	k.p.h.	miles per hour	m.p.h.
		meters per second	m.p.s.	feet per second	f.p.s.

2. GENERAL SYMBOLS

W, Weight $= mg$

g, Standard acceleration of gravity $= 9.80665$ m/s^2 or 32.1740 ft./sec.^{2}

m, Mass $= \frac{W}{g}$

I, Moment of inertia $= mk^2$. (Indicate axis of radius of gyration k by proper subscript.)

μ, Coefficient of viscosity

ν, Kinematic viscosity

ρ, Density (mass per unit volume)

Standard density of dry air, 0.12497 kg-m^{-4}-s^2 at 15° C. and 760 mm; or 0.002378 lb.-ft.$^{-4}$-sec.^{2}

Specific weight of "standard" air, 1.2255 kg/m^3 or 0.07651 lb./cu.ft.

3. AERODYNAMIC SYMBOLS

S, Area

S_w, Area of wing

G, Gap

b, Span

c, Chord

$\frac{b^2}{S}$, Aspect ratio

V, True air speed

q, Dynamic pressure $= \frac{1}{2}\rho V^2$

L, Lift, absolute coefficient $C_L = \frac{L}{qS}$

D, Drag, absolute coefficient $C_D = \frac{D}{qS}$

D_o, Profile drag, absolute coefficient $C_{D_o} = \frac{D_o}{qS}$

D_i, Induced drag, absolute coefficient $C_{D_i} = \frac{D_i}{qS}$

D_p, Parasite drag, absolute coefficient $C_{D_p} = \frac{D_p}{qS}$

C, Cross-wind force, absolute coefficient $C_C = \frac{C}{qS}$

R, Resultant force

i_w, Angle of setting of wings (relative to thrust line)

i_t, Angle of stabilizer setting (relative to thrust line)

Q, Resultant moment

Ω, Resultant angular velocity

$\rho\frac{Vl}{\mu}$, Reynolds Number, where l is a linear dimension (e.g., for a model airfoil 3 in. chord, 100 m.p.h. normal pressure at 15° C., the corresponding number is 234,000; or for a model of 10 cm chord, 40 m.p.s. the corresponding number is 274,000)

C_p, Center-of-pressure coefficient (ratio of distance of *c.p.* from leading edge to chord length)

α, Angle of attack

ϵ, Angle of downwash

α_o, Angle of attack, infinite aspect ratio

α_i, Angle of attack, induced

α_a, Angle of attack, absolute (measured from zero-lift position)

γ, Flight-path angle

REPORT No. 539

INVESTIGATION OF FULL-SCALE SPLIT TRAILING-EDGE WING FLAPS WITH VARIOUS CHORDS AND HINGE LOCATIONS

By RUDOLF WALLACE
Langley Memorial Aeronautical Laboratory

1347—35——1

NATIONAL ADVISORY COMMITTEE FOR AERONAUTICS

HEADQUARTERS, NAVY BUILDING, WASHINGTON, D. C.

LABORATORIES, LANGLEY FIELD, VA.

Created by act of Congress approved March 3, 1915, for the supervision and direction of the scientific study of the problems of flight. Its membership was increased to 15 by act approved March 2, 1929. The members are appointed by the President, and serve as such without compensation.

TECHNICAL COMMITTEES

AERODYNAMICS
POWER PLANTS FOR AIRCRAFT
AIRCRAFT STRUCTURES AND MATERIALS

AIRCRAFT ACCIDENTS
INVENTIONS AND DESIGNS

Coordination of Research Needs of Military and Civil Aviation

Preparation of Research Programs

Allocation of Problems

Prevention of Duplication

Consideration of Inventions

LANGLEY MEMORIAL AERONAUTICAL LABORATORY

LANGLEY FIELD, VA.

Unified conduct, for all agencies, of scientific research on the fundamental problems of flight.

OFFICE OF AERONAUTICAL INTELLIGENCE

WASHINGTON, D. C.

Collection, classification, compilation, and dissemination of scientific and technical information on aeronautics.

REPORT No. 539

INVESTIGATION OF FULL-SCALE SPLIT TRAILING-EDGE WING FLAPS WITH VARIOUS CHORDS AND HINGE LOCATIONS

By Rudolf Wallace

SUMMARY

An investigation was conducted in the N. A. C. A. full-scale wind tunnel on a small parasol monoplane equipped with three different split trailing-edge wing flaps. The object of the investigation was to determine and correlate data on the characteristics of the airplane and flaps as affected by variation in flap chord, flap deflection, and flap location along the wing chord. The chords of the flaps were 10, 20, and 30 percent of the wing chord and each flap was tested at deflections from 0° to 75° when located successively at 68, 80, and 88.8 percent of the wing chord aft of the leading edge. The investigation included force tests, pressure-distribution tests, and downwash surveys. The results give the lift, the drag, and the pitching-moment characteristics of the airplane, the flap forces and moments, the pressure distribution over the flaps and wing at one section, and the downwash characteristics of the flap and wing combinations.

An increase in flap chord or distance of the flap from the leading edge of the wing increased the lift of the airplane but had an adverse effect on the wing pitching moment. The L/D ratio of the airplane decreased with increase in flap deflection or flap chord. Flap normal-force coefficients were primarily a function of flap deflection and were relatively independent of flap chord, hinge-axis location, and airplane attitude. The location of the flap center of pressure in percentage of flap chord aft of the hinge axis remained practically constant irrespective of airplane attitude and of flap deflection, chord, or location. Flap hinge-moment coefficients varied with a power of flap chord greater than the square so that with regard to hinge moments narrow flaps were the most efficient in producing a given increase in lift.

Split trailing-edge flaps materially affected the magnitude and distribution of pressures over the entire wing profile. At low angles of attack the predominant effect of the flaps was to increase positively the lower-surface pressures; at high angles of attack, to increase negatively the upper-surface pressures. Downwash surveys indicated that horizontal tail planes located above the wing chord line would be more effective than those below the chord in counteracting the increased diving moment of the airplane with flaps deflected.

INTRODUCTION

The National Advisory Committee for Aeronautics has been active during the past 2 years in the investigation and development of split trailing-edge flaps as a device for improving the landing characteristics of high-speed aircraft and thereby increasing the safety of flight. Split trailing-edge flaps have been likewise investigated during this same period by various other research agencies and by aircraft manufacturers and have proved to be of such practical value that they are now accepted as a definite factor in contemporary aircraft design.

The accurate design and stress analysis of airplanes incorporating split trailing-edge wing flaps require that complete and coordinated data be available on all pertinent flap characteristics and properties, such as the effect of the flaps on the lift, drag, and pitching-moment characteristics of the airplane, the force and moment characteristics of the flaps, and the pressure distribution and downwash properties of the flap and wing combinations. Fairly complete data (references 1 to 5) are now available on the aerodynamic characteristics of model wings and of full-scale airplanes equipped with split flaps; somewhat limited data (reference 6) have also been presented on flap forces and moments. No information is available, however, as to the effect of split flaps on downwash or pressure distribution over a wing, and the existing force and moment data have been determined mostly from tests of small-scale models.

This report presents the results of tests conducted in the N. A. C. A. full-scale wind tunnel on a Fairchild 22 airplane equipped with split trailing-edge wing flaps. A conventional wing with an N. A. C. A. 2212 airfoil section was modified so that flaps having chords 10, 20, and 30 percent of the wing chord could be tested at deflections up to 75° with their hinge axes located at 3 positions along the wing chord. The investigation included force tests, pressure-distribution tests, and air-flow surveys. From the force and pressure-distribution tests were determined: the lift, drag, and pitching moment of the airplane; the normal force and center of pressure of the wing and of the flap at one section; and the normal force, center of pressure, and hinge

moment of the total flap. The air-flow surveys included measurements of downwash angles and of dynamic pressures in the region of usual tail-plane locations.

APPARATUS

Airplane.—The Fairchild 22 is a small open 2-place parasol monoplane powered with an inverted

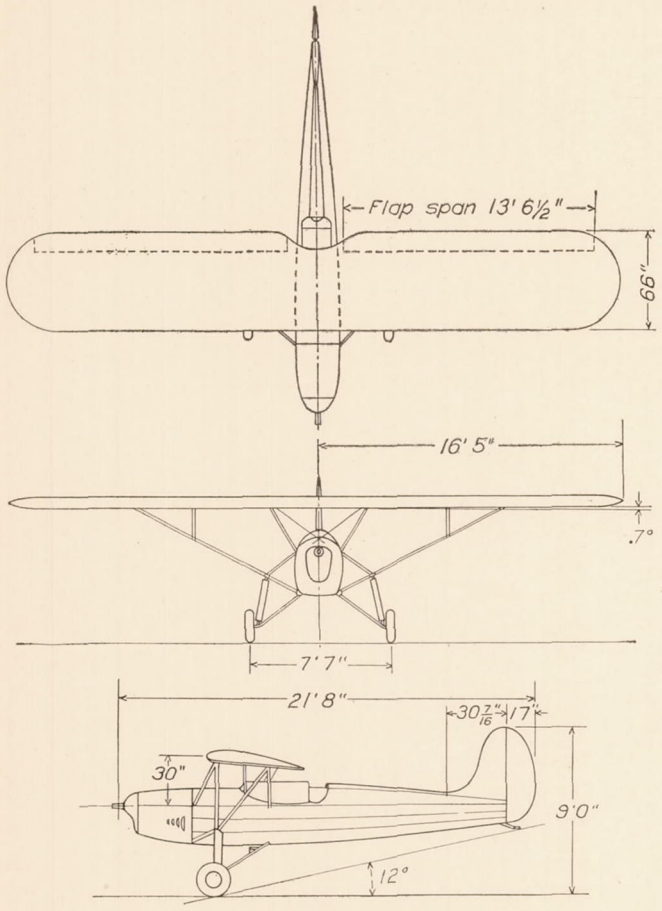

FIGURE 1.—The modified Fairchild 22 airplane.

Cirrus air-cooled engine. A 3-view drawing of the airplane is shown in figure 1; the principal characteristics of the airplane are given in table I.

The wing is of conventional wood and fabric construction with a span of 32 feet 10 inches and a chord of 66 inches. It has rounded tips, a center section cut-out at the trailing edge, and an N. A. C. A. 2212 airfoil section. The wing was modified for these tests by removing the trailing edge aft of the rear spar over the portion of the span normally utilized for ailerons and substituting therefor a special trailing-edge assembly. This assembly, consisting of a wooden spar, wooden ribs, and sheet-metal upper surface, was bolted directly to the rear spar of the wing so that the surface faired smoothly into the wing profile. A special rib to support the pressure orifices was built into the starboard wing without altering the airfoil section. The location of this pressure rib and the orifices thereon are shown in figure 2. In reference 7 is given a detailed description of the type of orifice used and the manner of its installation.

The plywood flaps were ⅝-inch thick and were attached to 2-inch bolting strips by piano hinges extending along the entire flap span. The 3 flap chords were

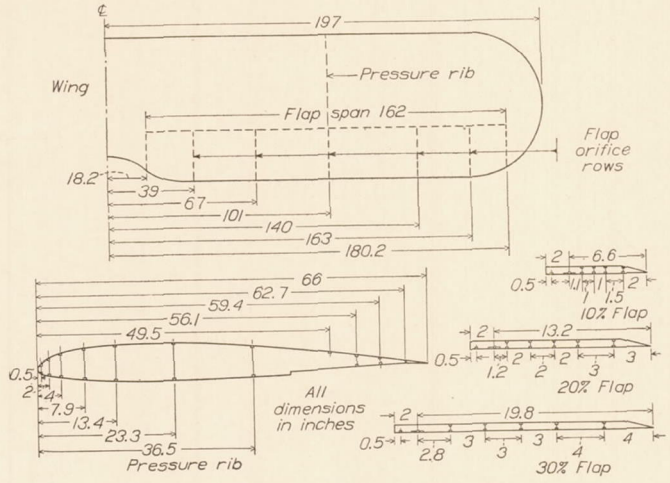

FIGURE 2.—Location of pressure orifices on wing and flap.

6.6 inches, 13.2 inches, and 19.8 inches, corresponding respectively to 10, 20, and 30 percent of the nominal wing chord. The spans of the flaps were identical, being 13 feet 6 inches, or 82.2 percent of the wing semispan, and each was slightly rounded at the ends to fair into the wing plan form. Pressure orifices were installed only in the starboard flaps and consisted of ⅛-inch copper tubes coming flush and fair with the

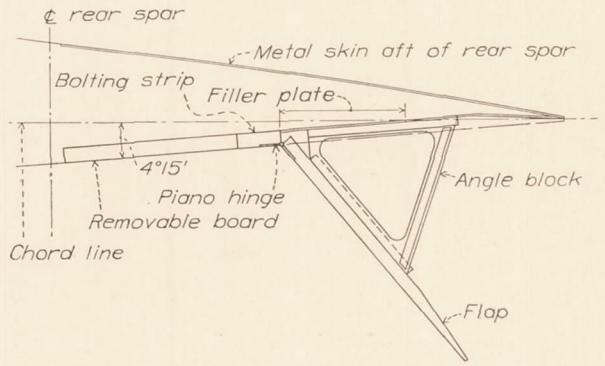

FIGURE 3.—Wing trailing edge and flap assembly.

flap surface. The location of the pressure orifices in each flap is shown in figure 2.

Figure 3 shows the modified trailing edge and a flap as assembled for testing. Six angle blocks maintained the flap angle along the span; boards and filler plates of varying width were used ahead of and behind the flap to complete the assembly for the different hinge-axis locations. A photograph of the wing with the 20-percent flap hinged at 80 percent of the wing chord and deflected 60° is shown in figure 4.

Manometer.—The manometer was of the multitube liquid type and provided simultaneous photographic records of 100 individual pressures at each exposure. A detailed description of its design and operation is given in reference 8. The manometer was installed in the front cockpit on pivots so that it would remain level as the angle of attack of the airplane was changed. The pressure orifices were connected to the manometer through aluminum and rubber tubing carried through the wing to the center line of the airplane and thence down a streamline strut to the front cockpit. The cockpits were covered to protect the manometer and to reduce the over-all drag of the set-up.

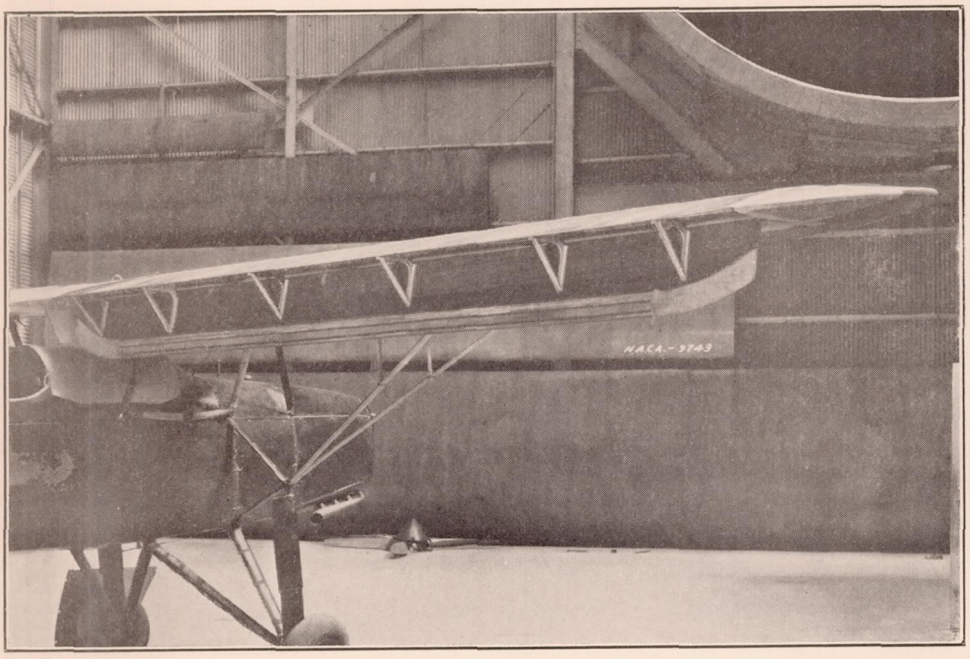

FIGURE 4.—View of wing with 20 percent c flap, hinged at 80 percent c and deflected 60°.

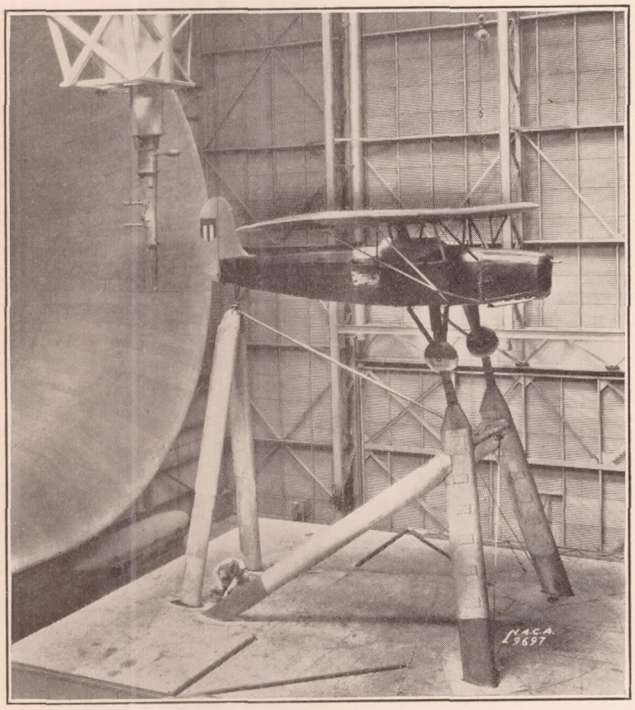

FIGURE 5.—The Fairchild 22 airplane mounted on the balance with the survey apparatus in the test position.

Wind tunnel and survey apparatus.—The N. A. C. A. full-scale wind tunnel and the survey apparatus are described in detail in reference 9. Figure 5 shows the Fairchild 22 airplane mounted on the balance with the survey apparatus in test position.

TESTS

All tests were conducted with the propeller and the horizontal tail surfaces removed and with the airplane set at 0° in roll and yaw. The wing was set 5° to the thrust axis. The tests were conducted at a dynamic pressure of approximately 8 pounds per square foot, corresponding at standard sea-level conditions to a velocity of 56 miles per hour and to a Reynolds Number of 2,880,000 based on the wing chord.

The lift, drag, and pitching moment of the airplane were determined over an angle-of-attack range from −16° to 20° for all flap conditions. The 10 and 20 percent c flaps were each tested at hinge-axis locations 68.0, 80.0, and 88.8 percent of the wing chord aft of the wing leading edge; the 30 percent c flaps were tested at the 68.0- and 80.0-percent hinge locations. Flap deflections, or the angular displacement of the flap from its closed position, varied from 0° to 75°. The 30 percent c flap was not tested at deflections greater than 40° nor in the rearmost position because of strength limitations of the airplane wing and structure. A summary of all flap conditions tested is given in the following table:

THE FLAP DEFLECTIONS, DOWNWARD, IN DEGREES, FOR THE FLAP ARRANGEMENTS TESTED

Flap chord percent c \ Hinge axis percent c aft L. E.	68	80	88.8
10	20 40 60	20 40 60 75	20 40 60
20	20 40 60	[a] 0 10 [a] 20 [a] 40 [a] 60 75	20 40 60
30	[b] 0 20 40	10 20 40	

[a] Downwash surveys.
[b] Hinge axis 70 percent c aft L. E.

Pressure readings were taken for all flap conditions at 7 angles of attack in the range from −12° to 12°. Each reading recorded the distribution of pressure over the flap at 5 sections along the span and over the wing at 1 section; 4 readings were taken at each test point to minimize the effect of rapid local air-flow fluctuations.

Downwash angle and dynamic-pressure surveys were made at 4 angles of attack in the range from −7° to 13° with the 20 percent c flap hinged at 80 percent of the chord and deflected 0°, 20°, 40°, and 60°. The surveys were conducted in a vertical plane extending directly downstream from the pressure rib and for each angle of attack the survey points were chosen to cover the area in which horizontal tail surfaces are normally located.

COEFFICIENTS

The results corrected for wind-tunnel effects are given in table II and presented in curve form in figures 6 to 24. The following coefficients are used:

$$C_L=\frac{L}{qS}$$

$$C_D=\frac{D}{qS}$$

$$C_m=\frac{M}{q\bar{c}S}$$

$$C_{N_w}{}'=\frac{N_w'}{qc}$$

$$C_{m_{c/4}}{}'=\frac{M_{c/4}'}{qc^2}$$

$$C_{N_F}{}'=\frac{N_F'}{qc_F}$$

$$C_{N_F}=\frac{N_F}{qS_F}$$

$$C_H{}'=\frac{M_H'}{qc^2}$$

where L and D are the lift and drag of the airplane, M is the pitching moment of the airplane about its center of gravity, N_w' is the pressure load on a flap and wing section of unit span normal to the wing chord, $M_{c/4}'$ is the moment about the quarter-chord point of the wing of a flap and wing section of unit span, N_F' is the pressure load on a flap section of unit span normal to the flap chord, N_F is the total pressure load of the flap normal to the flap chord, M_H' is the hinge moment of a flap section of unit span, q is the dynamic pressure, S is the wing area, S_F is the flap area, c is the wing chord, $\bar{c}$ is the mean wing chord, and c_F is the flap chord. Downwash characteristics are presented in terms of downwash angle, the deflection of the air stream from the horizontal (X) wind axis, and the ratio q_w/q, where q_w is the dynamic pressure in the wake and q is the dynamic pressure of the free air stream.

RESULTS OF FORCE TESTS

LIFT, DRAG, AND PITCHING MOMENT OF THE AIRPLANE

The curves of lift, drag, and pitching-moment coefficient shown in figure 6 present the corrected experimental results of the force tests and indicate the effect of flap arrangement on the aerodynamic characteristics of the Fairchild 22 airplane as tested with the horizontal tail surfaces removed. The lift curves for all combinations of flap deflection, flap chord, and hinge-axis location have similar characteristics in that the slopes are nearly constant and the stall occurs at approximately the same angle of attack. The increase in lift effected by the flaps results from a shift of the lift curves to the left on the scale of angle of attack, the magnitude of the displacement increasing with increase in flap deflection, flap chord, and distance of the hinge axis from the leading edge of the wing. Two minor variations are noted in the slopes of the lift curves. The slope increases as the hinge axis is moved toward the trailing edge of the wing and decreases as the flaps are deflected beyond a certain angle. This latter effect occurs at relatively small deflections with wide flaps so that the optimum flap angle, or the deflection that will give the greatest increase in $C_{L_{max}}$, becomes smaller as the flap width increases. The following table gives approximate values of $C_{L_{max}}$, for the Fairchild 22 airplane with simple split flaps of varying chord deflected to their respective optimum angles.

Flap chord in percent c of plain wing	Hinge axis in percent c	Flap deflection in degrees	$C_{L_{max}}$	Percentage increase in $C_{L_{max}}$
			1.46	
10	90	80	1.95	33.5
20	80	65	2.06	41.1
30	70	50	2.17	48.6

Split flaps increase the drag of the Fairchild 22 airplane so as greatly to reduce the ratio of L/D at

high angles of attack. At flap deflections above the optimum lift angle the drag continues to increase but the lift tends to decrease so that for extreme flap deflections the "air brake" action of the flaps becomes predominant.

The pitching-moment coefficients C_m shown in figure 6 indicate primarily the effect of split flaps on the pitching moment of the wing about the center of gravity of the airplane. In general, the diving moment of the wing increases with increase in flap deflection, flap chord, and distance of the hinge axis from the leading edge of the wing. The magnitude of this increase in diving moment is influenced somewhat by the general arrangement of the Fairchild 22 because the drag of the parasol wing produces an appreciable positive pitching moment about the center of gravity of the airplane. Were the wing located in a lower position with respect to the center of gravity, the flaps would produce a greater increase in diving moment. In the case of a complete airplane with horizontal tail surfaces in place, the foregoing increase in diving moment of the wing would be balanced in part by a concurrent positive increase in tail pitching moment due to greater angles of downwash at the tail. The degree to which these two moment increments may balance each other and thereby give a small resultant change in airplane pitching moment is dependent upon both the flap and tail-plane arrangements. The flap arrangement determines the increase in lift (and thereby, the change in downwash angle) and the increase in wing diving moment; the tail-plane arrangement (size and location with respect to the wing) determines the effect on tail moments of a change in downwash angle. Large diving moments would be expected, for instance, for an airplane with small tail surfaces poorly located behind a wing having a flap arrangement that gave a relatively large change in wing pitching moment and small increase in lift.

COMPARISON OF FLAP ARRANGEMENTS AT HIGH ANGLES OF ATTACK

Figures 7, 8, and 9 are included to illustrate the effect of the various flap arrangements on the aerodynamic characteristics of the Fairchild 22 airplane under landing conditions. An angle of attack of 12° was chosen to represent such conditions, a fair comparison of the flap arrangements at a higher angle of attack being unfeasible because of the erratic stalling characteristics of the airplane.

The curves of C_L and of L/D shown in figure 7 indicate the effect of flaps on the gliding characteristics of the Fairchild 22 airplane. The ability of an airplane to land safely in small fields or in those surrounded by obstacles is defined by its maximum available gliding angle and minimum flight-path velocity. As the gliding angle and flight-path velocity are inverse functions of L/D and C_L, it is desirable in landing to have a low L/D ratio in conjunction with a high value of $C_{L_{max}}$. The curves in figure 7 show that, for the Fairchild 22, an increase in flap width will both decrease the flight-path velocity and steepen the gliding angle. Moving the hinge axis toward the trailing edge of the wing would reduce the flight-path velocity but would not greatly affect the angle of glide.

The effect of flaps on pitching moment is of particular interest under landing conditions through its influence on the trimming characteristics of the airplane. The most desirable flap arrangement would be one that would afford a maximum improvement in lift and L/D with a minimum change in airplane pitching moments. The results of the force tests do not show directly the effect of flaps on airplane pitching moment but, for any given increase in lift, the change in downwash angle at the tail and the tail pitching-moment increment would be approximately the same irrespective of flap arrangement. The difference in wing pitching-moment increments for the various flap arrangements would therefore indicate, at a given value of lift increase, the effect on airplane pitching moment of a change in flap variable. A comparison of the different flap arrangements is presented on this basis in figure 8 by curves of ΔC_m plotted against ΔC_L. Inspection of the curves indicates that narrow flaps and those located toward the leading edge of the wing would effect a given increase in lift with a minimum negative increase in wing pitching moment and would therefore normally have the least effect on airplane pitching moments.

Comparative curves of lift coefficient, L/D ratio, and pitching-moment coefficient derived from the force test results are presented in figure 9 for two of the more commonly used types of flap, the simple split flap and the Zap flap. The simple split flap rotates about a fixed hinge axis so located that the trailing edge of the flap and wing coincide when the flap is closed. The Zap flap moves rearward when deflected, the trailing edge of the flap traveling on a line perpendicular to the wing chord line at the wing trailing edge.

Curves are shown in figure 9 for a Zap flap of 20 percent c chord and for simple split flaps of 10, 20, and 30 percent c chords. For a split flap of given chord width the Zap arrangement will give a higher maximum lift than will a simple split flap but will have a more adverse effect on wing pitching moment. An increase in chord width for simple split flaps will give an increase in lift and a reduction in L/D ratio with practically no change in wing pitching moment. This latter result may at first appear to be inconsistent with the results previously discussed but, in reality, an increase in chord for simple split flaps involves two flap variables: flap chord and hinge-axis location. It is evident that as the chord of the flap is increased the hinge axis must shift forward to maintain the trailing edge of the flap

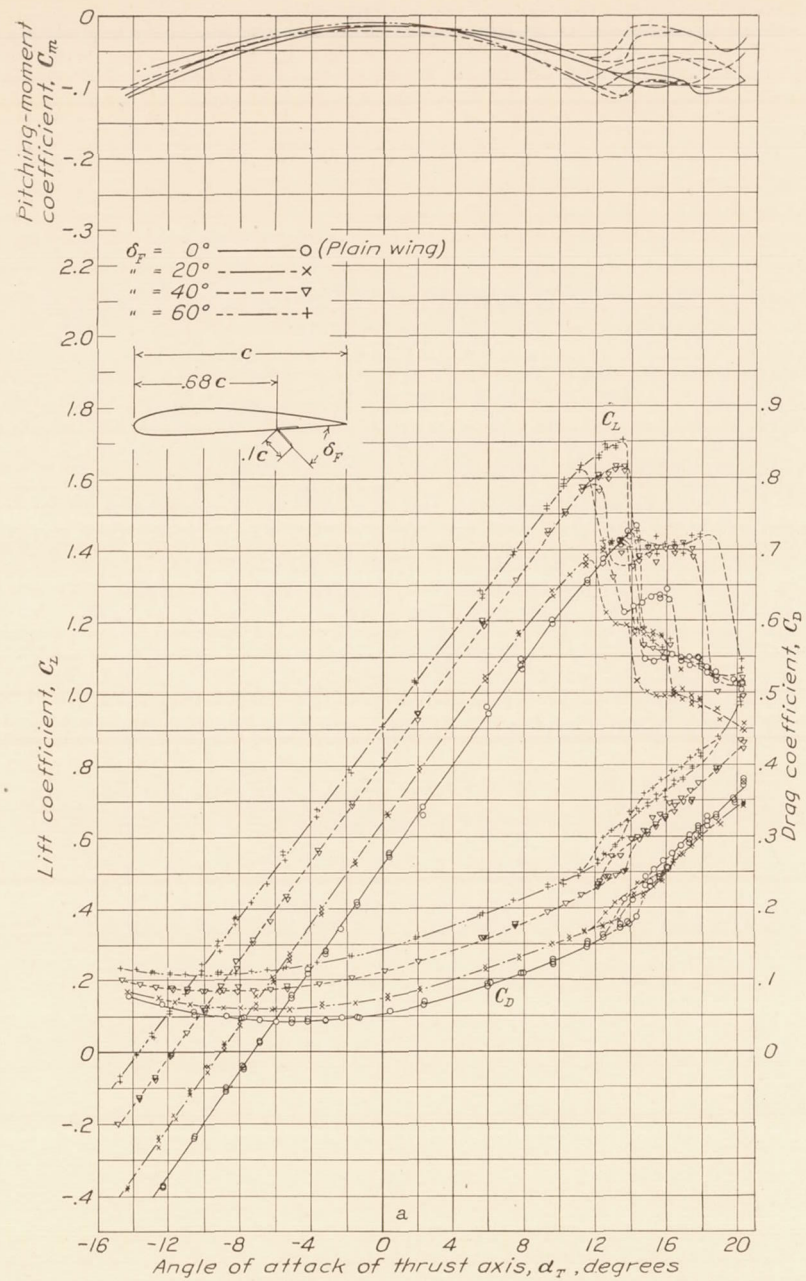

(a) The 10 percent c flap hinged at 68 percent c.

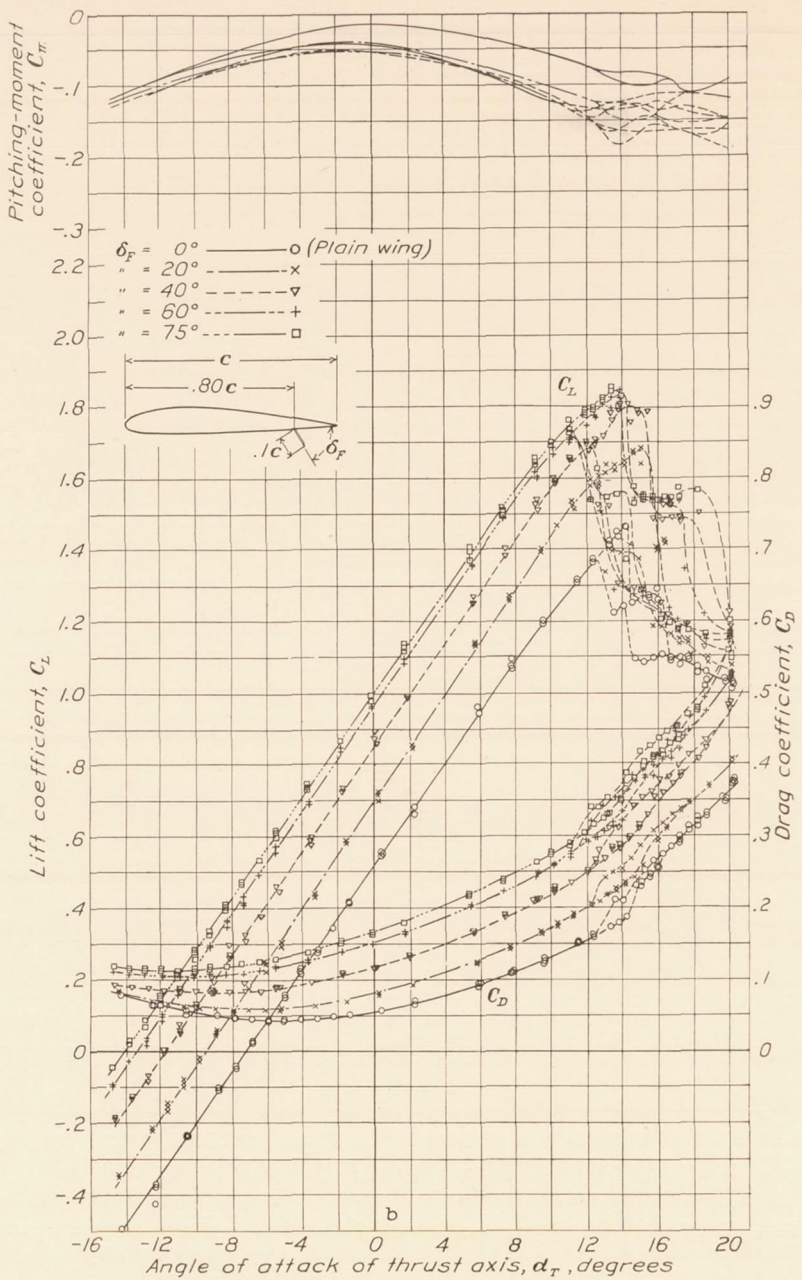

(b) The 10 percent c flap hinged at 80 percent c.

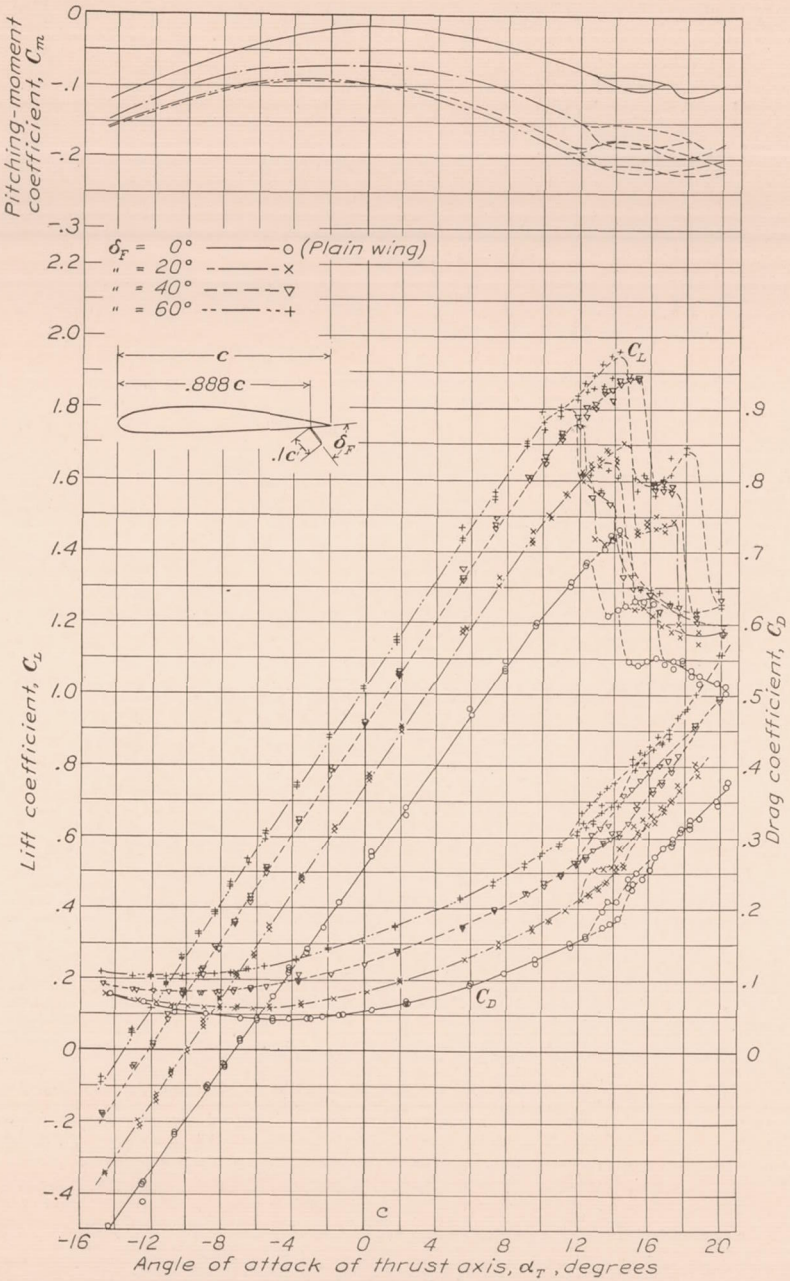

(c) The 10 percent c flap hinged at 88.8 percent c.

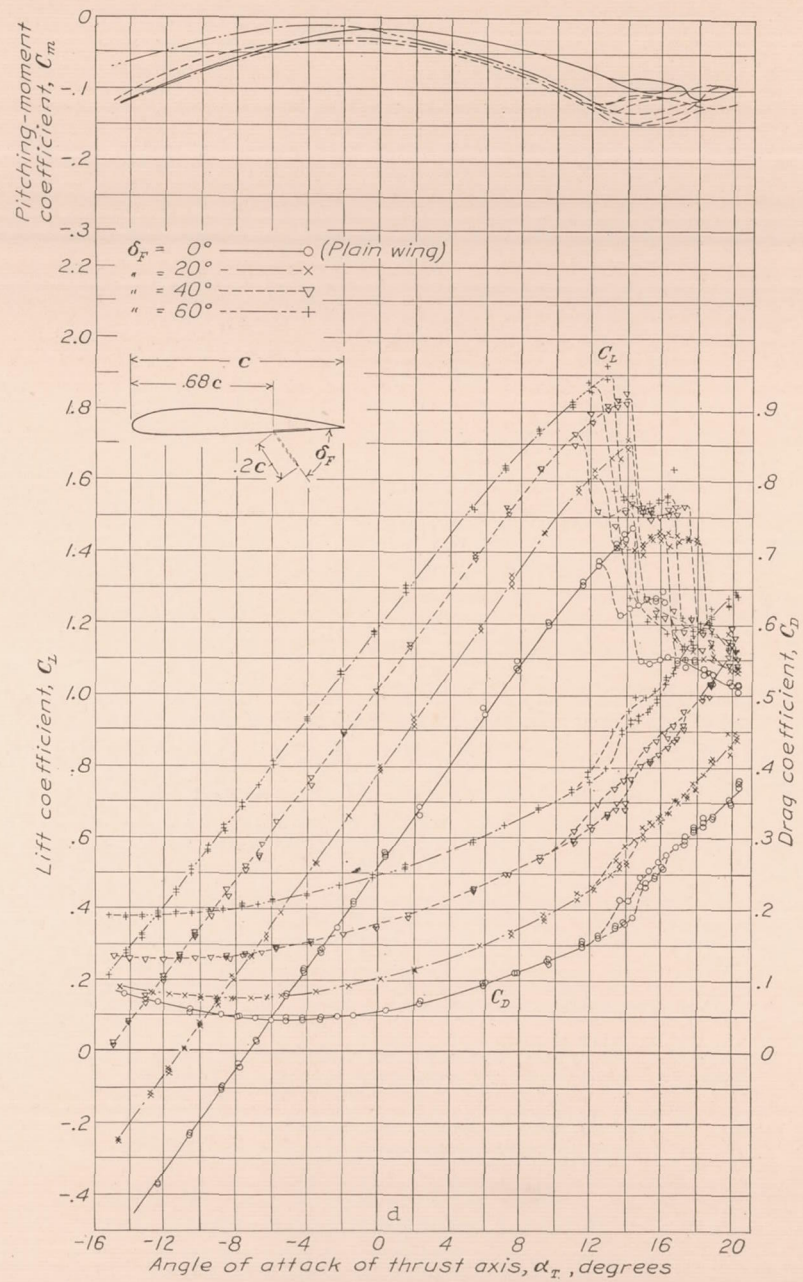

(d) The 20 percent c flap hinged at 68 percent c

FIGURE 6.—Lift, drag, and pitching-moment coefficients of the Fairchild 22 airplane with split trailing-edge wing flaps.

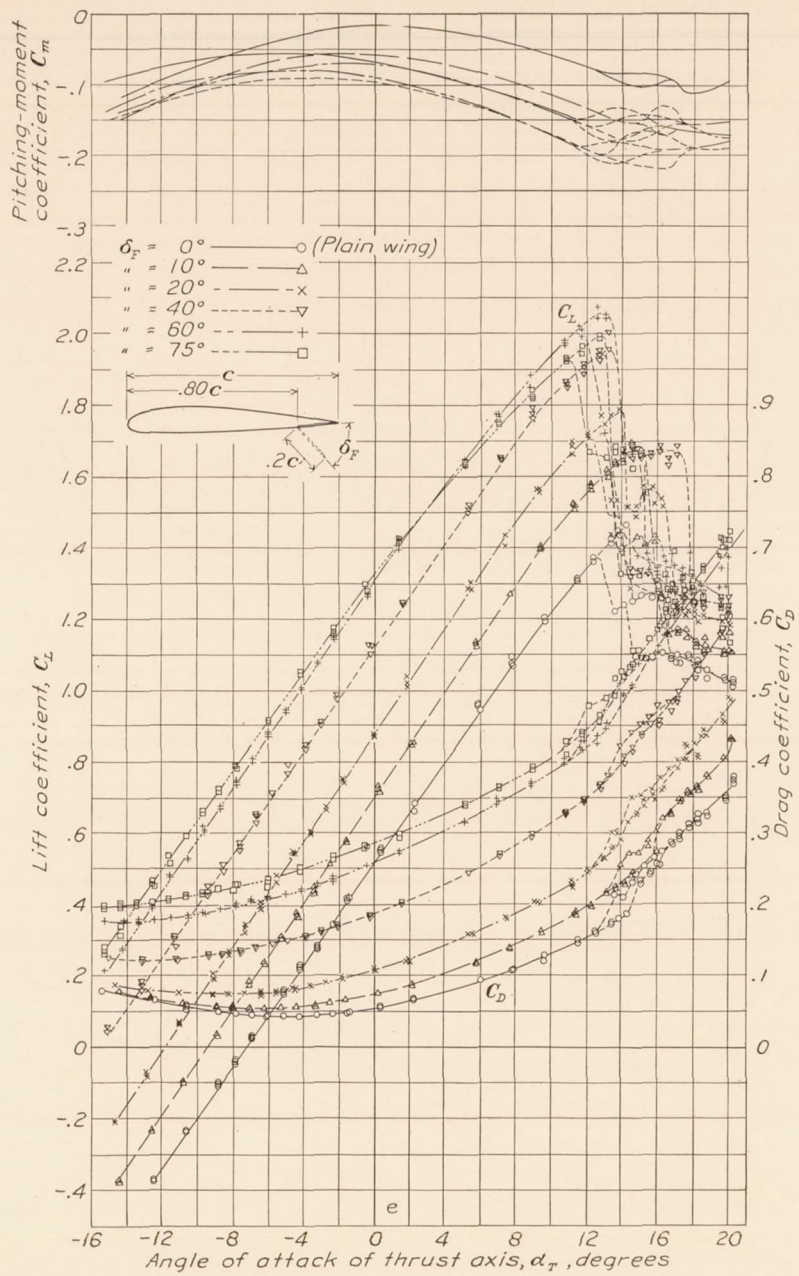

(e) The 20 percent c flap hinged at 80 percent c.

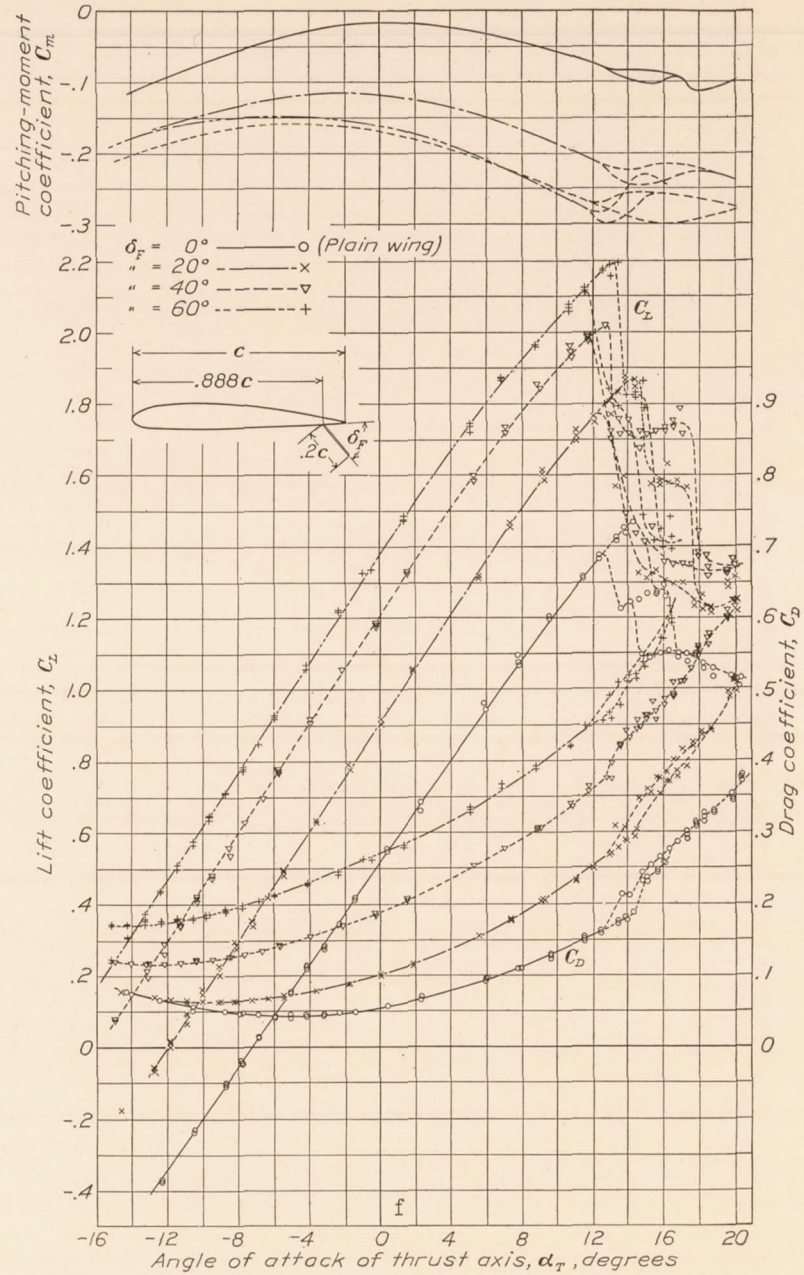

(f) The 20 percent c flap hinged at 88.8 percent c.

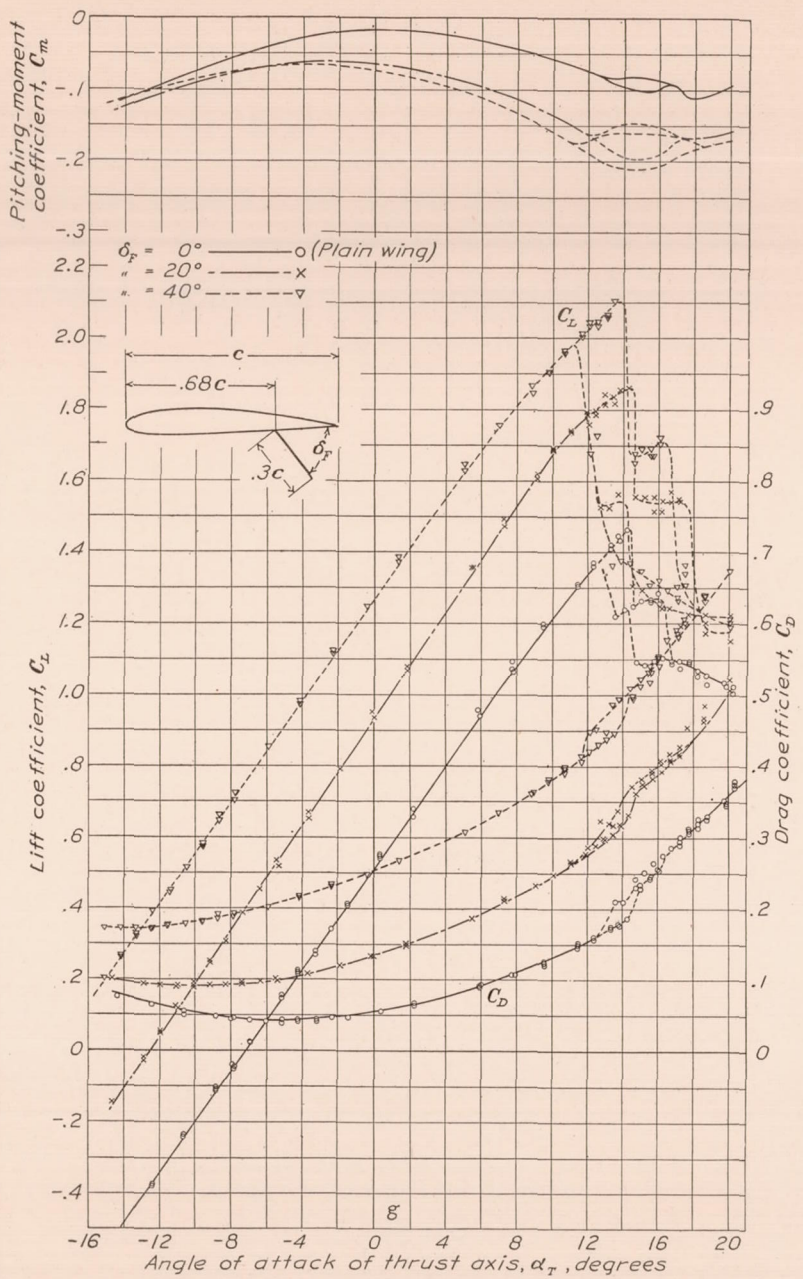

(g) The 30 percent c flap hinged at 68 percent c.

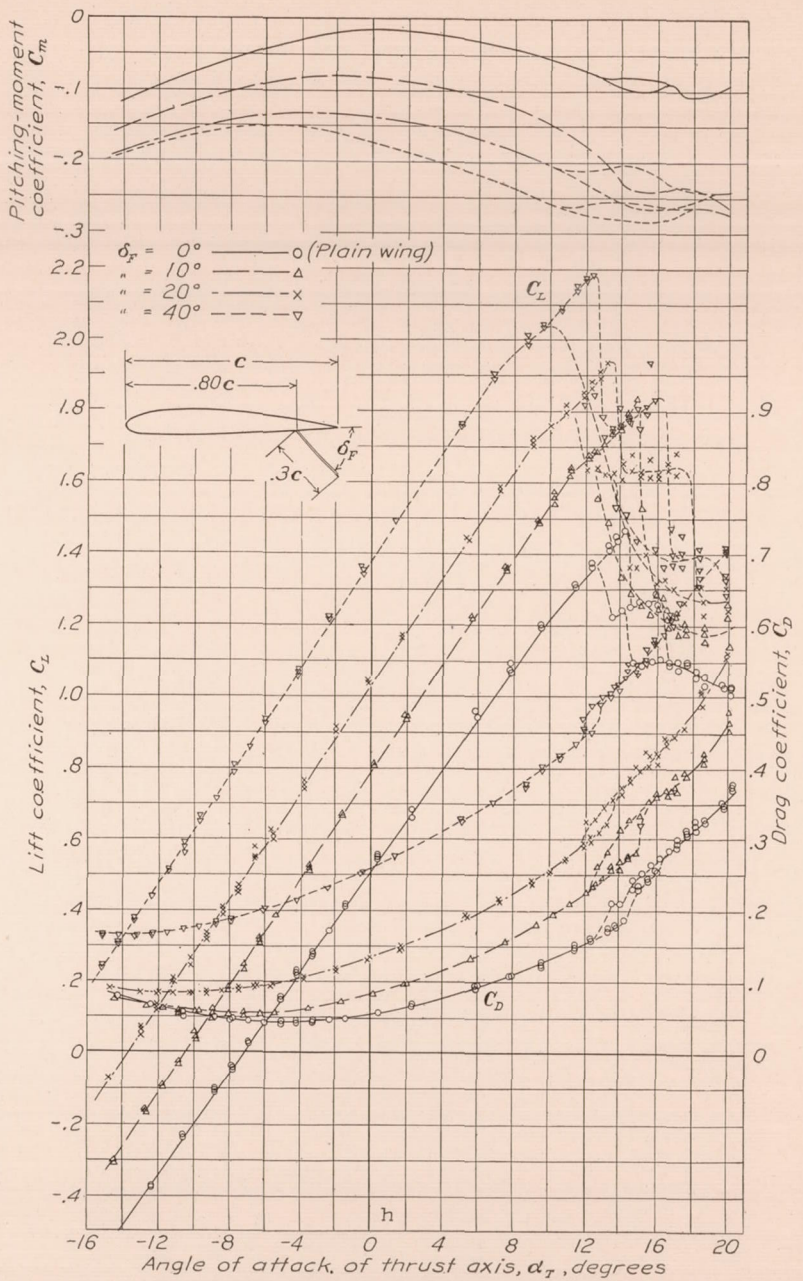

(h) The 30 percent c flap hinged at 80 percent c.

FIGURE 6.—Continued. Lift, drag, and pitching-moment coefficients of the Fairchild 22 airplane with split trailing-edge wing flaps.

and wing coincident at zero deflection. As these two variations in flap arrangement affect the pitching

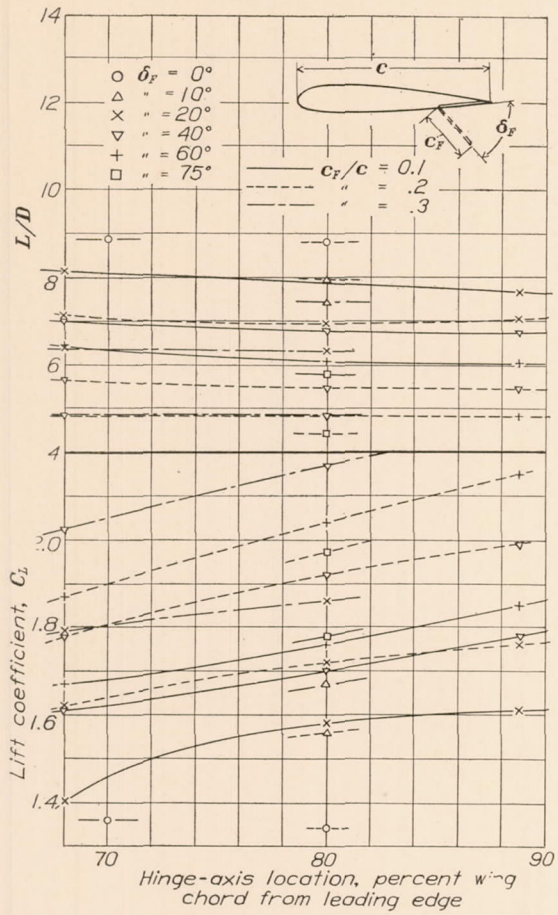

FIGURE 7.—Summary of lift and L/D of Fairchild 22 airplane with split trailing edge flaps at α_T=12°.

moment of the airplane in a sense of opposite sign and approximately equal magnitude, the resultant change

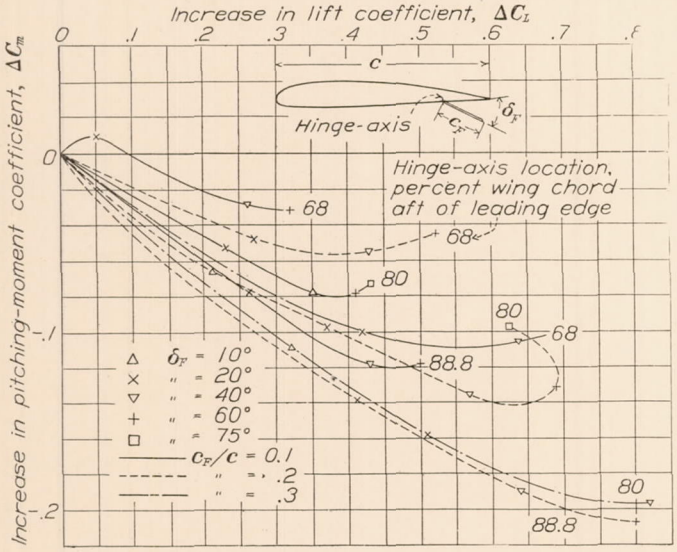

FIGURE 8.—Variation of ΔC_m with ΔC_L for Fairchild 22 airplane with split trailing-edge wing flaps at α_T=12°.

in pitching moment is relatively small. An increase in chord width for simple split flaps would therefore be distinctly advantageous insofar as the effect on the aerodynamic characteristics of the airplane is concerned. The reduction in flight velocity and increase in angle of glide that could be realized by increasing the chord may, however, be limited by structural considerations imposed by the force and hinge-moment characteristics of the wider flaps.

WING LIFT AND DRAG INCREMENTS

The results presented in figures 6 to 9 are directly applicable only to the Fairchild 22 airplane, the co-

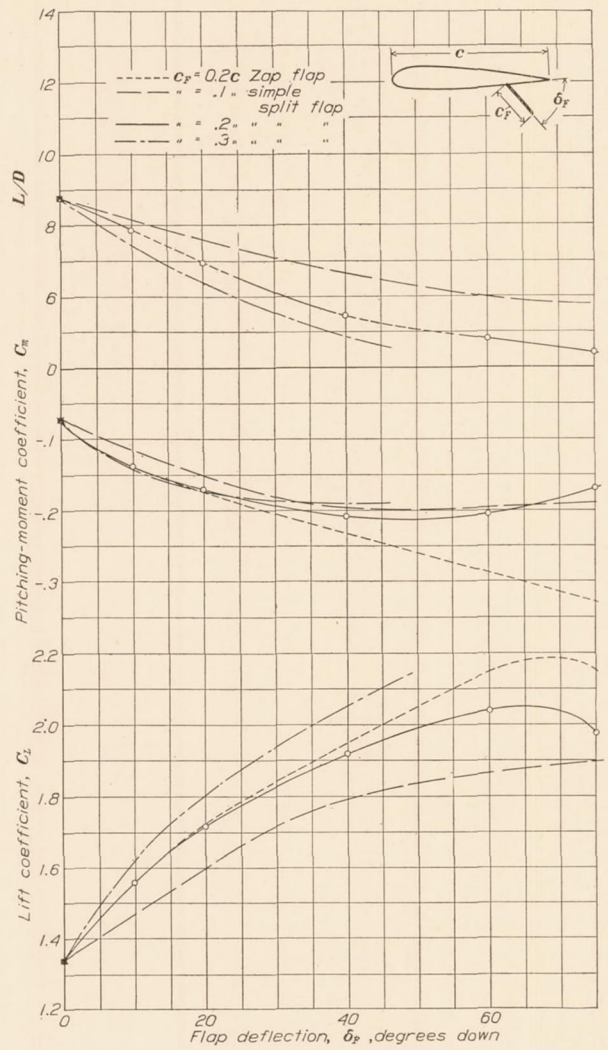

FIGURE 9.—Lift, L/D, and pitching moments for Fairchild 22 airplane with Zap flap and with simple split flap at α_T=12°.

efficients having been determined from the forces acting on the entire airplane. At a given angle of attack, however, it is reasonable to assume that the change in lift and drag of the airplane results entirely from the effect of the flaps on the wing characteristics, as the forces acting on the remainder of the airplane should be practically independent of flap arrangement. On the basis of this assumption, the changes in wing lift and drag for the various flap arrangements were determined from the curves of figure 6 and are presented in figures 10 and 11 as curves

of ΔC_L and ΔC_D plotted against angle of attack of the wing. These coefficient increments are believed to be directly additive for wings of a section similar in thickness and camber to that of the N. A. C. A.

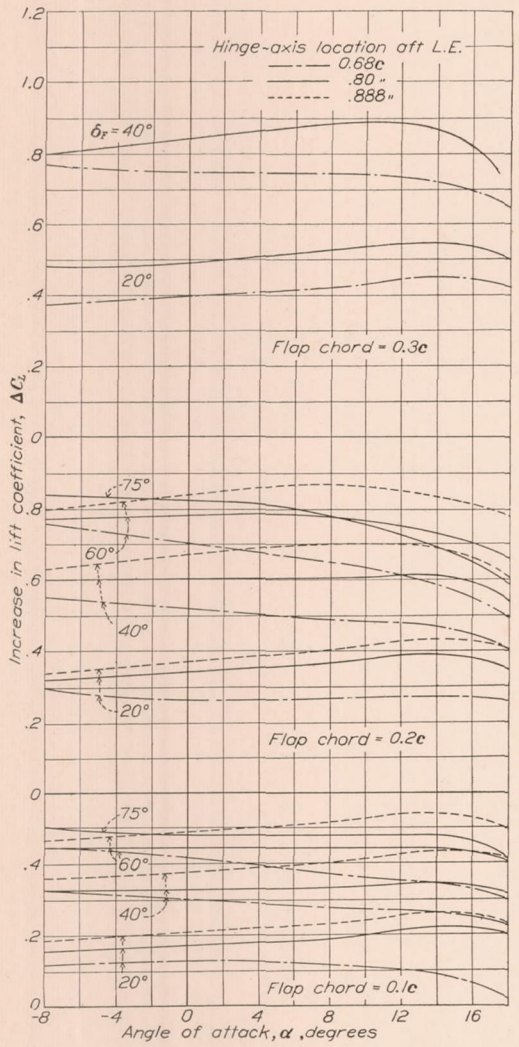

FIGURE 10.—Increase in lift coefficient of Fairchild 22 wing for various split-flap arrangements.

2212. Allowance has not been made in the values of ΔC_L and ΔC_D for the fact that the flaps did not extend over the entire span of the wing nor for the effect of the rounded wing tips and the circular cut-out of the center section.

The curves of coefficient increments (ΔC_L and ΔC_D) shown in figures 10 and 11 exhibit only one characteristic not previously indicated in the discussion of the effect of flaps on the lift and drag of the airplane. This characteristic is the decreasing influence of flap location on the value of the increments as the angle of attack is reduced. In particular, it is noted that ΔC_D becomes independent of hinge-axis location at negative angles of attack.

RESULTS OF PRESSURE-DISTRIBUTION TESTS

The results of pressure-distribution measurements taken about a section of the wing and flap are presented in table II and in figures 12 to 19. Typical plots of p/q against chord position are shown in figure 12 for the 20 percent c flap hinged at 80 percent c. Each point on the curve represents the average value of p/q from four pressure measurements taken at that orifice location. The pressure data given in table II and the section force and moment coefficients for the wing and flaps were obtained from the plots of figure 12 and from similar plots for the various other flap arrangements. Values of p/q are given in table II for the upper and lower surfaces at various stations along the wing and the flap chords. Complete data are given for the 20 percent c flap hinged at 80 percent c and sufficient

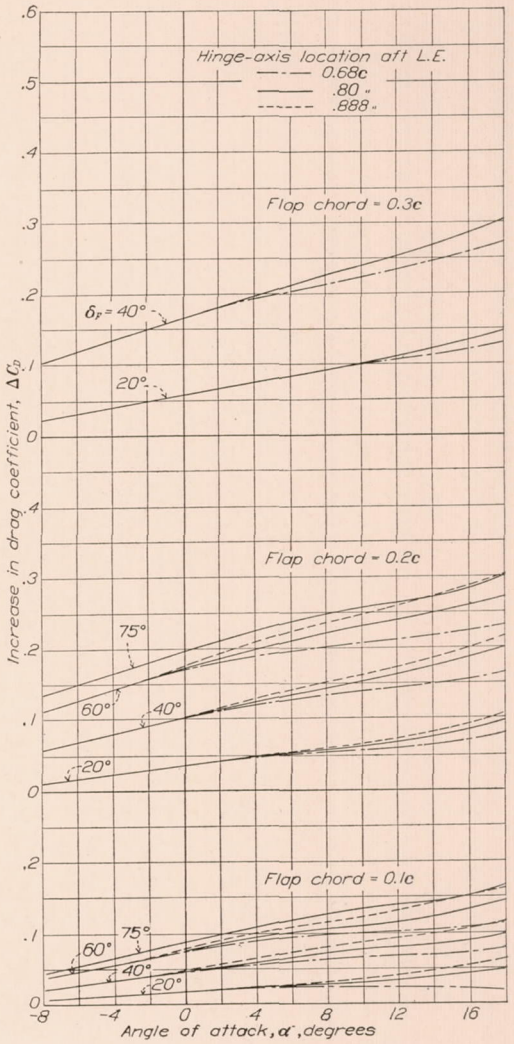

FIGURE 11.—Increase in drag coefficient of Fairchild 22 wing for various split-flap arrangements.

data are included for other hinge-axis locations and flap chords to illustrate the effect of these variables on the distribution of pressure about the flap and the wing section.

EFFECT OF FLAPS ON CHORD LOAD DISTRIBUTION

Split trailing-edge flaps materially affected the magnitude and distribution of pressures over both the

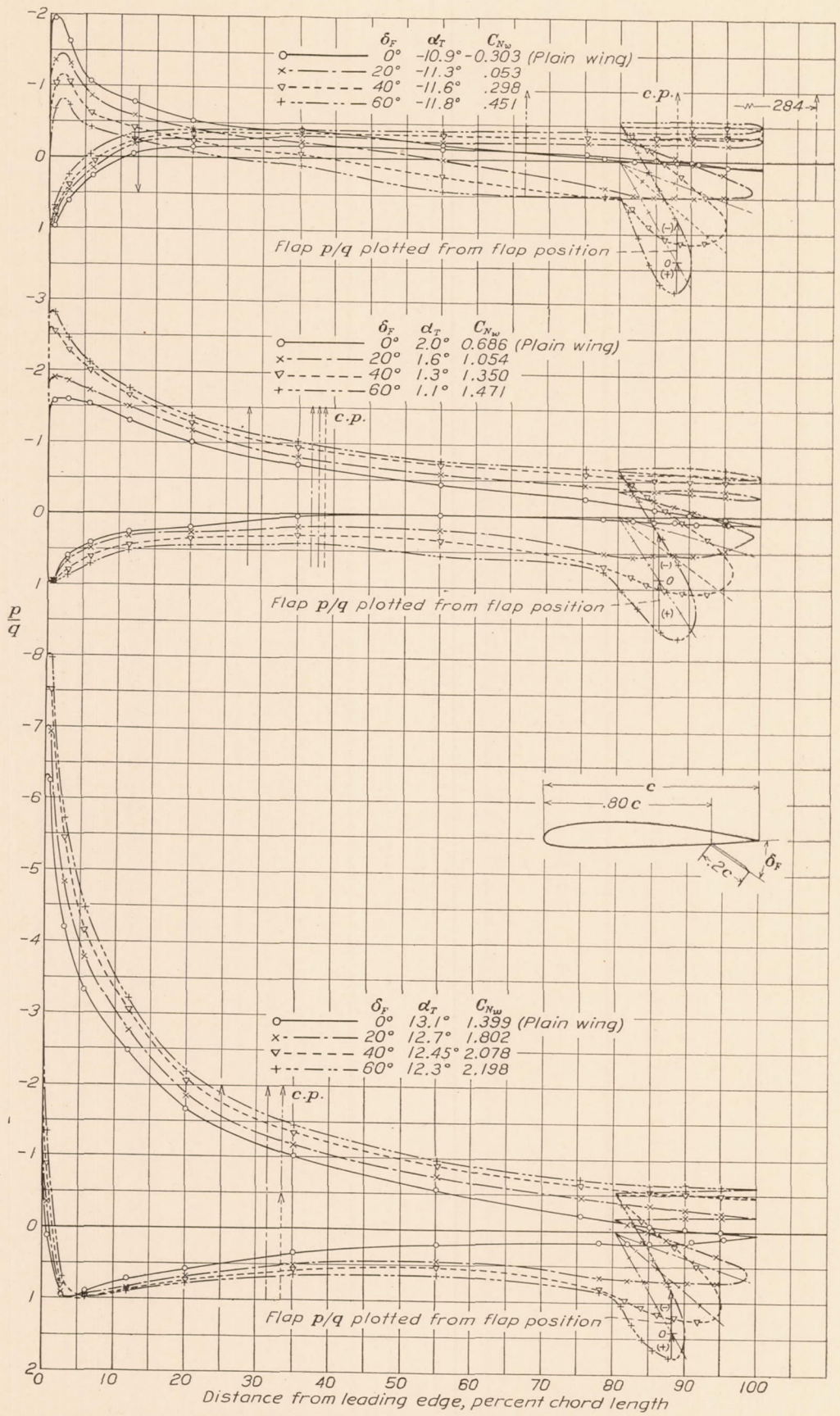

FIGURE 12.—Pressure distribution for wing with 20 percent c flap hinged at 80 percent c. Corrected for tunnel-wall effect.

upper and lower surfaces of the wing. As the flaps were depressed, an increase in pressure differential between the wing surfaces was effected in part by a negative increase of upper-surface pressures and in part

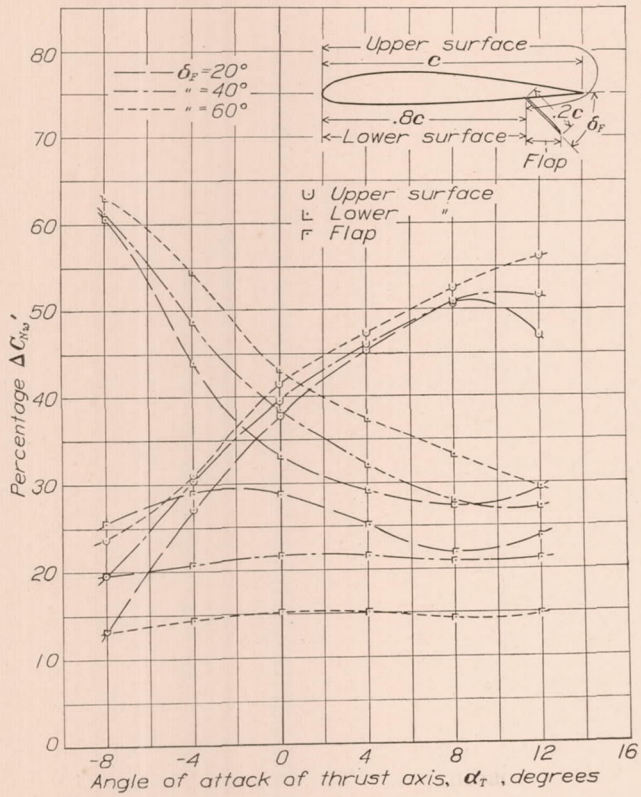

FIGURE 13.—Distribution of increase in normal-force coefficient ($\Delta C_{N_w}'$) between flap and wing surfaces for 20 percent c flap hinged at 80 percent c.

by a concurrent increase of positive lower-surface pressures. At a given flap deflection the pressure-differential increase remained essentially constant throughout the angle-of-attack range but an inspection of the p/q plots in figure 12 will show that the relative portions of this increase that can be attributed respectively to the upper and lower surfaces of the wing vary widely with angle of attack. This variation in pressure distribution with angle of attack is more clearly illustrated in figures 13 and 14 by curves that define independently the loading characteristics of the various lifting surfaces of the wing. The curves of figure 13 indicate the percentage of increase in normal-force coefficient ($\Delta C_{N_w}'$) carried by the upper surface of the wing, the lower surface, and the flap for an angle-of-attack range from −8° to 12°. The curves of figure 14 similarly define the percentage of wing normal-force coefficient (C_{N_w}') attributable to these respective surfaces. Although the curves in figures 13 and 14 present the surface loading characteristics only for the 10 percent c flap hinged at 80 percent c, they illustrate the general effect of split flaps on the distribution of pressure loads about the wing profile.

Reference to figure 13 shows that, at an angle-of-attack of −8°, approximately 60 percent of the increase in normal-force coefficient ($\Delta C_{N_w}'$) produced by the flaps comes from the increase in pressure loading on the lower surface of the airfoil and that the upper surface contributes only from 15 to 25 percent of $\Delta C_{N_w}'$. At high angles of attack this condition is reversed and the increase in pressure loading on the upper surface of the wing accounts for more than 50 percent of $\Delta C_{N_w}'$ and less than 30 percent of $\Delta C_{N_w}'$ can be attributed to an increase in lower-surface pressures. The increment in wing normal force derived from the pressures acting directly on the flaps is fairly constant over the angle-of-attack range but decreases with flap deflection. This latter effect results primarily from the reduction in projected area of the flap on the chord of the wing.

The distribution of $\Delta C_{N_w}'$ between the flap and upper and lower surfaces of the wing is also indicated

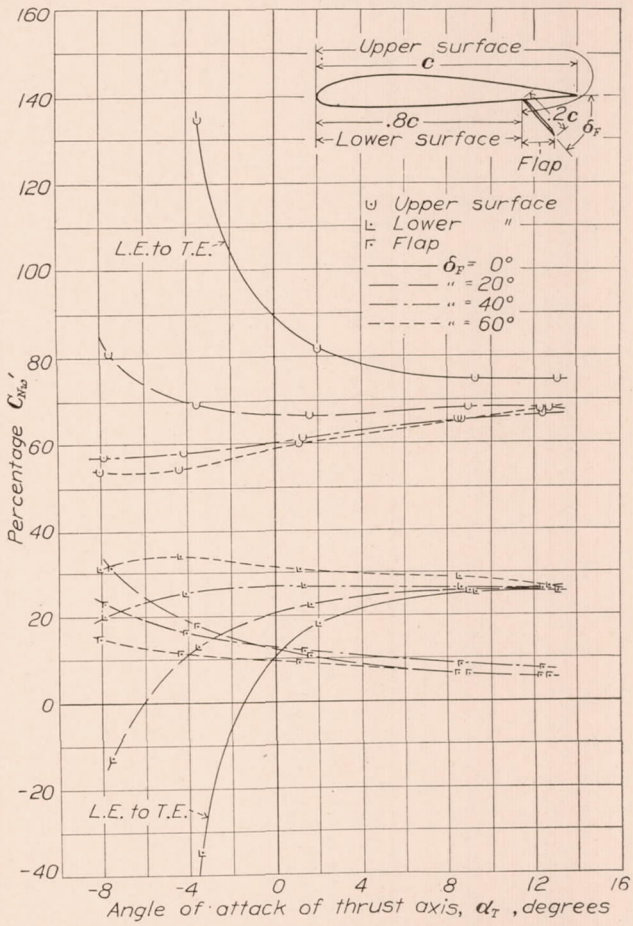

FIGURE 14.—Distribution of normal-force coefficient (C_{N_w}') between flap and wing surfaces for 20 percent c flap hinged at 80 percent c.

by the percentage of wing normal-force coefficient carried by each of these surfaces (fig. 13). At low angles of attack the percentage of wing normal force carried by the lower surface increases rapidly with flap deflection, and the percentage for the upper surface is correspondingly reduced. At high angles of attack, however, the variation in surface loads with flap deflection is comparatively small. As the flaps are de-

pressed, at an angle of attack of 12°, the percentage of wing normal-force coefficient carried by the lower surface of the wing remains essentially constant, and the upper-surface percentage is reduced only by the relatively small load carried directly on the flaps; that is, the increase in normal force with flap deflection is distributed between the upper and lower surfaces of the wing at high angles of attack in such proportions that, irrespective of flap deflection, the percentage of total

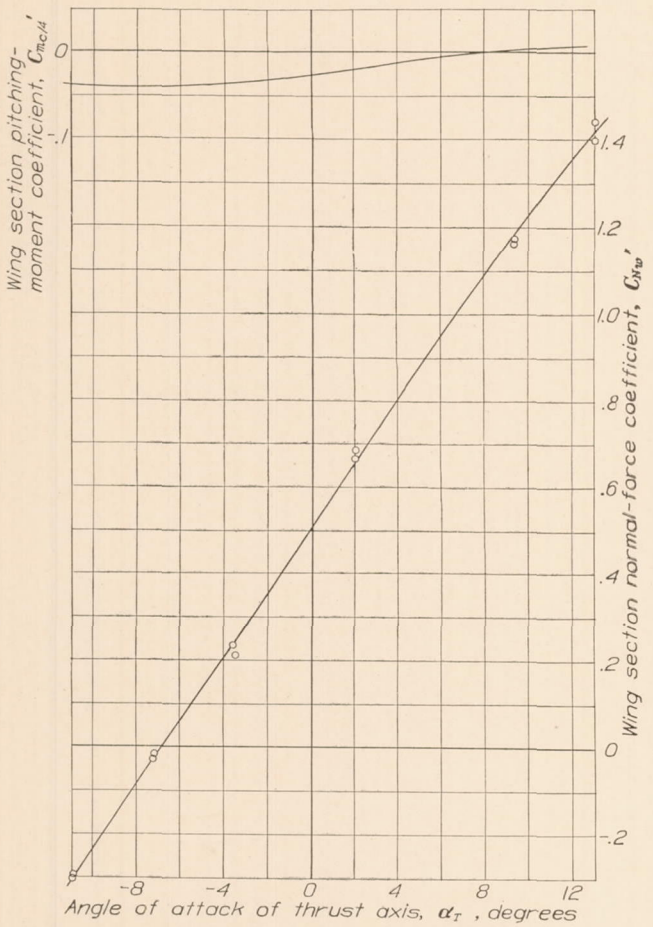

FIGURE 15.—Section normal-force and pitching-moment characteristics of the plain wing.

wing normal force carried by each remains roughly the same as for the plain wing.

At a given angle of attack and flap deflection an increase in flap chord does not alter the distribution of pressure about the wing profile but merely increases the pressures on both the upper and lower surfaces of the wing. Upper-surface pressures show only slight variations with change in hinge-axis location, and the increase in normal force and lift that occur when the hinge axis is moved toward the trailing edge of the wing results largely from the coincidental increase in effective lower-surface area.

The maximum negative pressure recorded in these tests was 8.7 q. This pressure occurred on the upper surface of the airfoil near the leading edge with the 20 percent c flap hinged at 80 percent c and deflected 75° at an angle of attack of 12.2°. This value represents an increase in negative pressure of 2.7 q over the maximum negative pressure for the plain wing at the same angle of attack. Positive lower-surface pressures approach 1 q near the hinge axis at large flap deflections and high angles of attack.

Although the leading edge of the wing is subject to the maximum absolute variations in pressures with flap deflection, the critical changes in loading occur near the trailing edge. It will be noted that the increment of pressure effected by the flaps is relatively uniform along the wing chord as compared with the initial pressure distribution of the plain wing. As this original distribution involves large pressures at the leading edge, decreasing to relatively small pressures at the trailing edge, it follows that the superposition of a uniform pressure increment on this initial distribution would result in comparatively large percentage increases in loading at the trailing-edge sections. Reference to figure 12 (20 percent c flap, hinged at 80 percent c) shows that at an angle of attack of approximately 12.5° a flap deflection of 60° increases the pressure load across a section at the 65 percent c station from 0.56 q to 1.52 q, or 172 percent. Further analysis likewise indicates that the moment of the trailing-edge loads about this 65 percent c station, which corresponds approximately to normal rear-spar locations, would be increased some 350 percent by a 60° deflection of the flap. This increase presupposes, of course, a constant value of q and, as flight velocities are normally reduced when the flaps are deflected, the increase in loads and moments would be correspondingly less. It should be emphasized, however, that the variation in pressures near the trailing edge is similar throughout the angle-of-attack range and therefore large loads and moments would occur in high-velocity dives or if the flaps were suddenly deflected during high-speed flight. The foregoing effects are accentuated by moving the flaps toward the trailing edge of the wing.

SECTION NORMAL-FORCE AND MOMENT CHARACTERISTICS OF WING AND FLAPS

The section characteristics of the wing and flaps as determined from integration of the pressure-distribution plots are presented in figures 15 to 19. Figure 15 shows the section normal-force coefficient and the pitching-moment coefficient about the quarter-chord point for the plain wing plotted against the angle of attack of the airplane. These curves serve to coordinate the section data with the remainder of the results and indicate the degree of accuracy of the pressure-distribution measurements. The points shown on the normal-force coefficient curve are for the initial test run made with the 20 percent c flap hinged at 80 percent c and for the final test run made with the 30 percent c flap hinged at 70 percent c, the flaps being closed in each case. The agreement of the

points is considered to be very good for pressure-distribution tests. The pitching-moment coefficients about the quarter-chord point for the plain wing were computed only from the normal force and the center-of-pressure location, the pitching moment due to pressure and shear forces parallel to the chord being neglected. The fact that the pitching-moment curve shown in figure 15 has an appreciable slope and therefore does not give an approximately constant value of $C_{m_{c/4}}'$, as would be expected for an N. A. C. A. 2212 airfoil section, indicates that the foregoing method of computing pitching moments does not give exactly corrrect results; but, as the pitching-moment characteristics of the wing with flaps were determined from similar computations and are presented in terms of the increase in pitching moment due to the flaps, it is believed that the results are satisfactorily accurate. The moment of the flap normal-force component parallel to the chord of the wing was included in computing the pitching moments for the wing with flaps.

The section normal-force and the hinge-moment characteristics of the flaps and the effect of the flaps on the normal-force and pitching-moment characteristics of the wing are presented in figure 16 by curves of C_{N_F}', C_H', $\Delta C_{N_w}'$, $(c.\ p.)_w'$, and $\Delta C_{m_{c/4}}'$ plotted against C_{N_w}' for the plain wing. At a given value of the normal-force coefficient of the plain wing these curves therefore define (for any of the flap arrangements tested) the normal-force and hinge-moment coefficients of the flap, the center-of-pressure location of the wing, and the increase in the normal-force and pitching-moment coefficients of the wing. It is believed that the relationships thus established would hold for other airfoil sections having a distribution of pressure similar to that of the N. A. C. A. 2212, i. e., having similar thickness and camber, and that, knowing the normal-force coefficient for such a section, the flap characteristics and the effect of the flaps on the wing characteristics can be determined from the curves of figure 16.

Deflection of split flaps to moderate angles produces an increase in wing normal force and shifts the center of pressure from the leading edge of the wing. Extreme deflections may reverse this relationship and result in a loss in wing normal force and a reduction in wing diving moment. The magnitude of flap normal-force coefficients is primarily a function of flap deflection and increases from approximately zero for the closed flaps to values of 1.3 or more for extreme flap angles. It follows that flap hinge moments likewise vary directly with flap deflections.

An increase in flap chord increases the normal force and diving moment of the wing and likewise increases the normal-force coefficient of the flap. Flap hinge moments, in particular, are influenced by flap width, the variation in hinge-moment coefficients being in excess of the square of the variation in flap width. Because of the extreme increase in hinge moment with increase in flap width, narrow flaps are much more efficient than wide ones in producing a given increase in wing normal force with the least control effort. (See fig. 17.) In consideration of the effect of hinge-moment characteristics on the required weight, strength, and mechanical advantage of the flap-operating mechanism, the results therefore indicate that the narrowest flap which will produce the desired or required lift, drag, and pitching-moment characteristics would be the most desirable.

Variation in flap hinge-axis location has little effect on flap forces or moments but has a marked influence on the wing characteristics. Wing normal force and diving moment decrease as the flaps are moved toward the leading edge of the wing. The value of $\Delta C_{m_{c/4}}'$ for a hinge-axis location of 68 percent c is from 30 to 60 percent of that for a hinge-axis location of 88.8 percent c. This decrease in $\Delta C_{m_{c/4}}'$ is considerably greater than the concurrent decrease in $\Delta C_{N_w}'$, which suggests that hinge-axis locations somewhat nearer the leading edge of the wing than those investigated in these tests would give reasonably large increases in wing normal force with a negligible effect on pitching moment.

The location of the center of pressure for split flaps in terms of percent flap chord aft of the hinge axis is essentially independent of flap chord, flap position, and angle of attack of the wing. The variation of flap center-of-pressure location with flap deflection is indicated by the curve of figure 18. Even this variation in center-of-pressure location is small and a value of 41 percent of the flap chord aft of the hinge axis may be considered as an approximate location for all the flap arrangements investigated in these tests.

TOTAL FLAP CHARACTERISTICS

The flap characteristics presented in figures 16, 17, and 18 are for a section approximately at the center of the flap span. Pressure measurements were taken at four other sections along the span of the flap and the characteristics of the total flap thereby determined. These results are presented in figure 19 by curves giving the ratio of total flap normal-force coefficient to section normal-force coefficient. These curves present average values for all flap chords and hinge-axis locations. The location of the center of pressure for the total flap is the same as for the flap section.

SUMMARY OF WING AND FLAP CHARACTERISTICS

A summary of important wing and flap characteristics as determined from both force and pressure distribution tests is given in the following table for an angle of attack of the wing of 17° (α_T=12°).

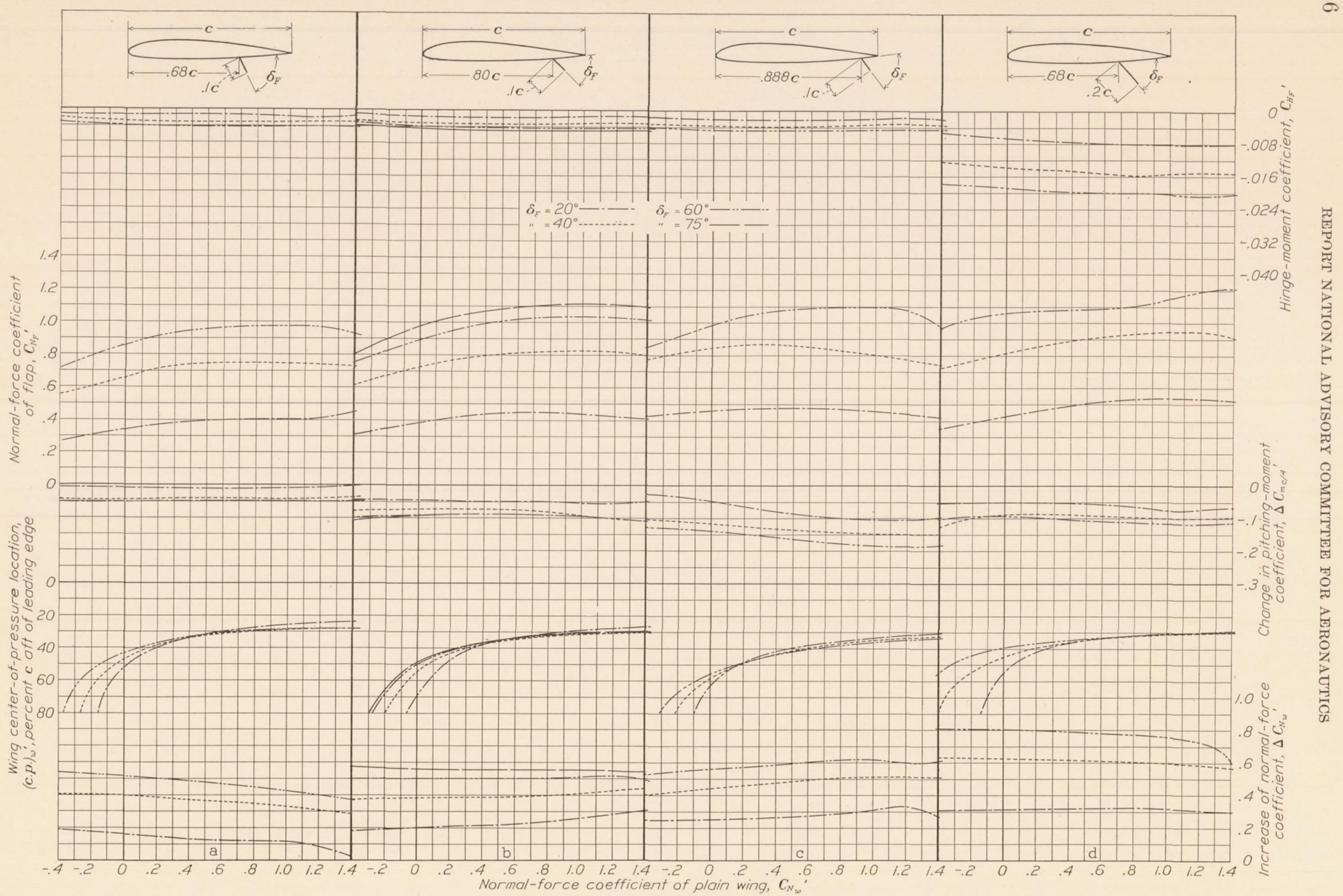

(a) The 10 percent c flap hinged at 68 percent c.

(b) The 10 percent c flap hinged at 80 percent c.

(c) The 10 percent c flap hinged at 88.8 percent c.

(d) The 20 percent c flap hinged at 68 percent c.

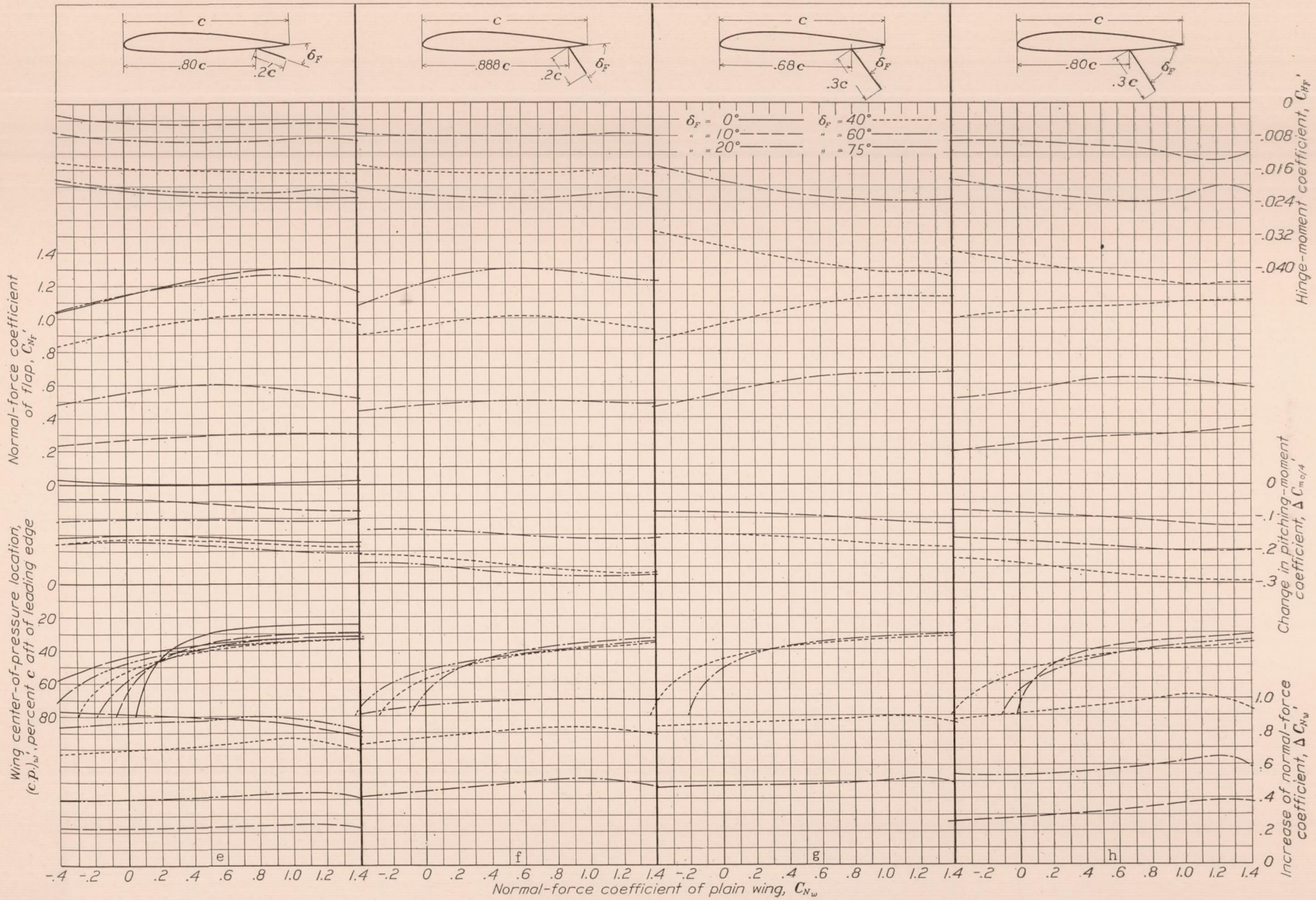

(e) The 20 percent c flap hinged at 80 percent c.

(f) The 20 percent c flap hinged at 88.8 percent c.

(g) The 30 percent c flap hinged at 68 percent c.

(h) The 30 percent c flap hinged at 80 percent c.

FIGURE 16.—Section normal-force and moment characteristics of wing and flaps.

c_F percent c	Hinge axis percent c aft L. E.	δ_F deg.	ΔC_L	ΔC_D	$\Delta C_{N_w}'$	$\Delta C_{m_{c/4}}'$	C_{N_F}'	C_H'
10	68	20	0.04	0.020	0.04	−0.01	0.43	−0.0016
		40	.24	.075	.29	−.04	.73	−.0030
		60	.31	.110	.38	−.05	.94	−.0043
	80	20	.21	.046	.30	−.05	.41	−.0015
		40	.33	.093	.44	−.11	.80	−.0031
		60	.42	.138	.50	−.11	1.02	−.0043
		75	.44	.158	.54	−.11	1.10	−.0050
	88.8	20	.25	.059	.29	−.10	.42	−.0018
		40	.43	.111	.51	−.15	.75	−.0032
		60	.51	.156	.60	−.19	1.01	−.0044
20	68	20	.26	.076	.30	−.07	.53	−.0082
		40	.43	.161	.57	−.10	.93	−.0151
		60	.52	.228	.67	−.12	1.21	−.0205
	80	20	.36	.092	.42	−.11	.53	−.0086
		40	.57	.195	.70	−.19	.98	−.0170
		60	.68	.267	.83	−.21	1.18	−.0212
		75	.62	.292	.79	−.18	1.31	−.0229
	88.8	20	.42	.102	.48	−.17	.48	−.0077
		40	.64	.209	.79	−.27	.93	−.0164
		60	.79	.296	1.00	−.28	1.23	−.0221
30	68	20	.43	.125	.50	−.12	.67	−.0234
		40	.67	.265	.87	−.19	1.13	−.0416
	80	10	.33	.070	.38	−.13	.34	−.0128
		20	.52	.140	.61	−.20	.59	−.0188
		40	.78	.295	.98	−.29	1.11	−.0436

RESULTS OF AIR-FLOW SURVEYS

The results of the air-flow surveys are presented in figures 20 to 23 by contours of downwash angle and the ratio of q_w/q plotted against distance from the trailing edge of the wing as measured in chord lengths along the wind axes. These contours define the wake characteristics in a plane intersecting the wing at approximately the center of the wing semispan. Because of the wide variation in both average downwash angles and in contour patterns for different planes along the wing span, these results are strictly indicative of wake characteristics only for the survey plane in which they were measured. In general, the downwash angles given by the contour plots are somewhat greater than those for planes closer to the center of the wing. The downwash survey results are also influenced by circulation phenomena arising from the fact that the flaps did not extend across the center section of the wing. With the flaps deflected, the span-loading curve for the wing is depressed at the center with a resultant shedding of a series of trailing vortices from the inner ends of the flaps. These trailing vortices reduce the effective aspect ratio of the wing and tend to increase the downwash angles in the survey plane.

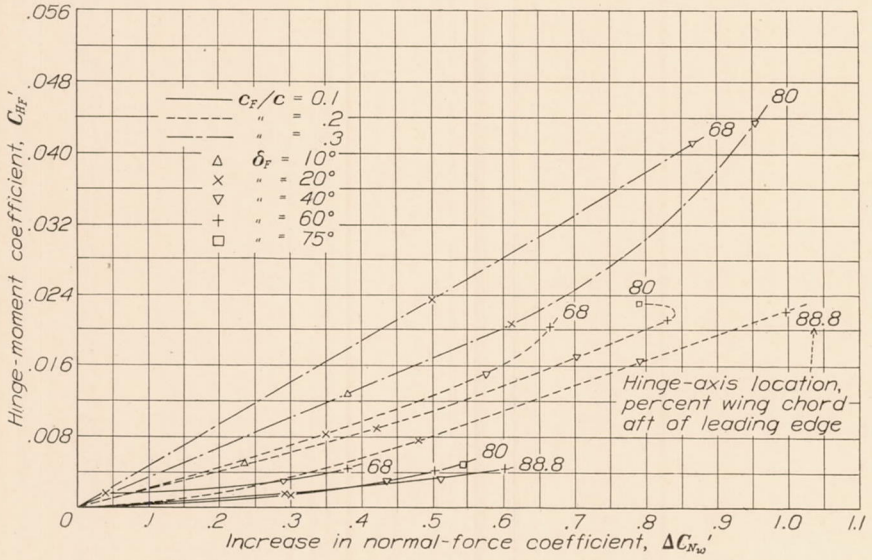

FIGURE 17.—Variation of C_{H_F}' with $\Delta C_{N_w}'$ for the wing section. C_{N_w}' for plain wing = 1.35.

COMPARISON OF CALCULATED AND MEASURED DOWNWASH ANGLES

Wake characteristics are defined by the downwash angles and the velocities existing in the rear of the wing. The value of the downwash angle ϵ at a given point in the wake is a function of the aspect ratio of the wing, the lift coefficient at which the wing is operating, and the location with respect to the wing of the point under consideration. Empirical equations that express the downwash angle in terms of these variables have been developed by Diehl and by Toussaint and, as these equations are commonly used for computing downwash angles, a comparison of the equations with the results of the downwash surveys may be of interest.

The equations developed by Diehl and by Toussaint are identical in form and give the downwash, respectively, for biplanes and monoplanes. Toussaint's equation for the downwash in the rear of a monoplane is

$$\epsilon=\frac{55.7C_L}{A}(x+1)^{-0.38}(y+1)^{-0.23}$$

where ϵ is the downwash angle in degrees.

A, the aspect ratio of the wing.

x, the distance in chord lengths from the trailing edge of the wing, parallel to the chord line, to any point in rear of the wing.

y, the perpendicular distance in chord lengths from the point to the extended chord line of the wing.

Values of ϵ computed from this equation for a lift coefficient of 1.42 are shown in figure 24 in the form of downwash-angle contours, which may be directly compared with those obtained from the air-flow surveys. Exact agreement could not be expected between the calculated and measured downwash angles, as Toussaint's equation is for the downwash in

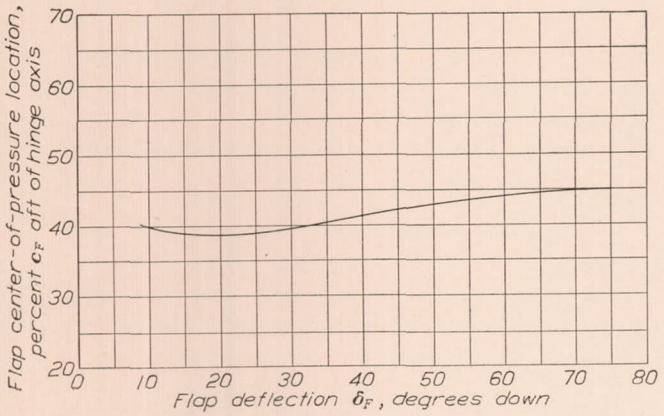

FIGURE 18.—Variation of flap center-of-pressure location with flap deflection.

the rear of the center of the wing; whereas the surveys were conducted in a plane at the center of the semispan. The disagreement between the contours, however, is too marked to be accounted for solely by the difference in span location. Also, other comparisons made between calculated values of ϵ based on this equation and downwash angles measured aft of the midspan section of a rectangular airfoil (unpublished data) have shown even greater discrepancies than do the contours in figure 24. In particular, Toussaint's assumption that the points of maximum downwash angle lie along the extended chord line of the wing is not substantiated by survey results, and the variation of downwash angle with vertical and horizontal distance from the wing is more pronounced than the equation indicates. From the general nature of the downwash contours it does not appear feasible to attempt the derivation of a more satisfactory empirical equation for computing downwash angle without more complete experimental data.

The contours shown in figure 24 also illustrate the effect on downwash characteristics of the discontinuity of the flaps at the center of the wing. The contours for the plain wing and for the wing with flaps depressed are for comparable values of C_L and should therefore be quite similar except for probably minor variations resulting from differences in energy loss in the wake due to profile drag. It is noted, however, that the downwash contours for the two conditions differ considerably both in average value of downwash angle and in contour pattern. These discrepancies are due primarily to the effect of the trailing vortices at the inner ends of the flaps.

VELOCITY DISTRIBUTION IN WAKE

In addition to the downwash angles existing in the rear of a wing, the wake is characterized by a region of reduced velocity, which results from inclusion in the downwash of air that has passed close to the wing and been subject to high viscous shearing forces. This core of low-velocity air is swept downward from the trailing edge of the wing by the downwash and is gradually dissipated through the accelerating action of the surrounding air stream. It appears logical that the velocity gradient in this core and the core width should bear some relationship to the profile drag of the lifting surface which creates it. For normal airfoil profiles the low velocities have largely disappeared at the distances in the rear of the wing at which horizontal tail planes are usually located but, in the case where the wing is equipped with such a high-drag device as split flaps, the survey results show that the ratio of q_w/q may be as low as 0.7 at two chord lengths aft of the trailing edge of the wing. It is therefore important that the tail planes operating in the downwash of a wing with split flaps should be so located with respect to the wing as to be outside the low-velocity region at all angles of attack of the airplane, particularly since this low-velocity region is also one of very turbulent and unstable air flow.

The location of the downwash core in the general wake pattern is determined primarily by the lift

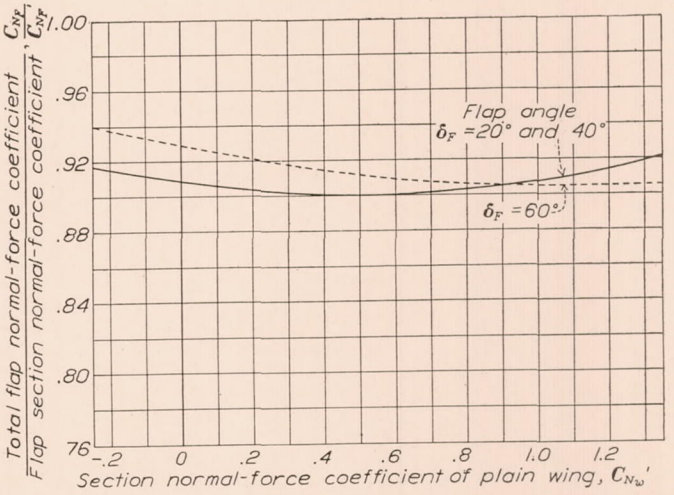

FIGURE 19.—Ratio of total flap normal-force coefficient to flap section normal-force coefficient.

coefficient at which the wing is operating, the higher the lift coefficient the greater the deflection of the core axis from the horizontal wind axis. In general, the line of minimum q_w/q lies slightly below the line of maximum downwash angle. As for downwash angles, no accurate empirical equation can be given defining the distribution of velocities in the wake.

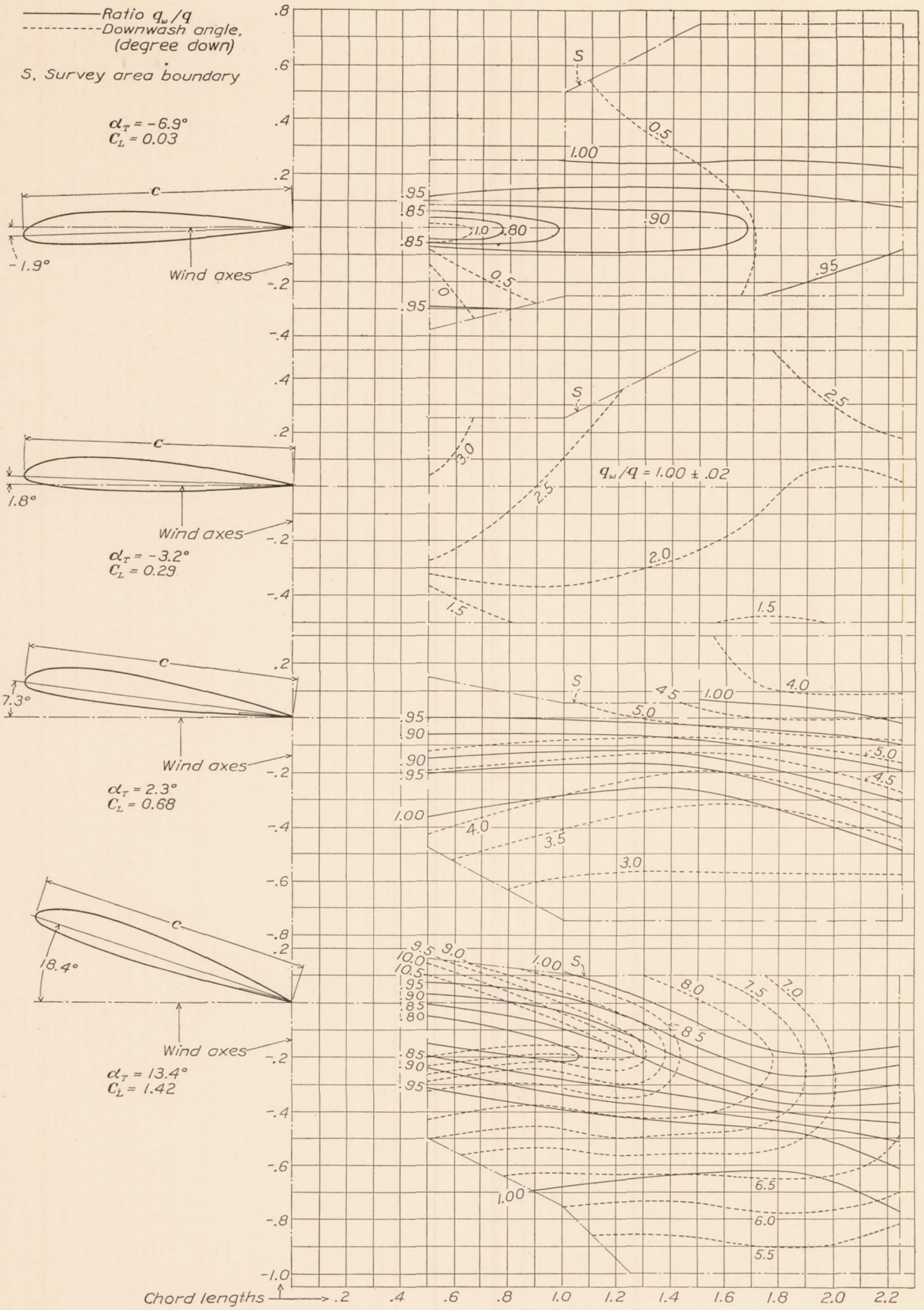

FIGURE 20.—Downwash contours for plain wing.

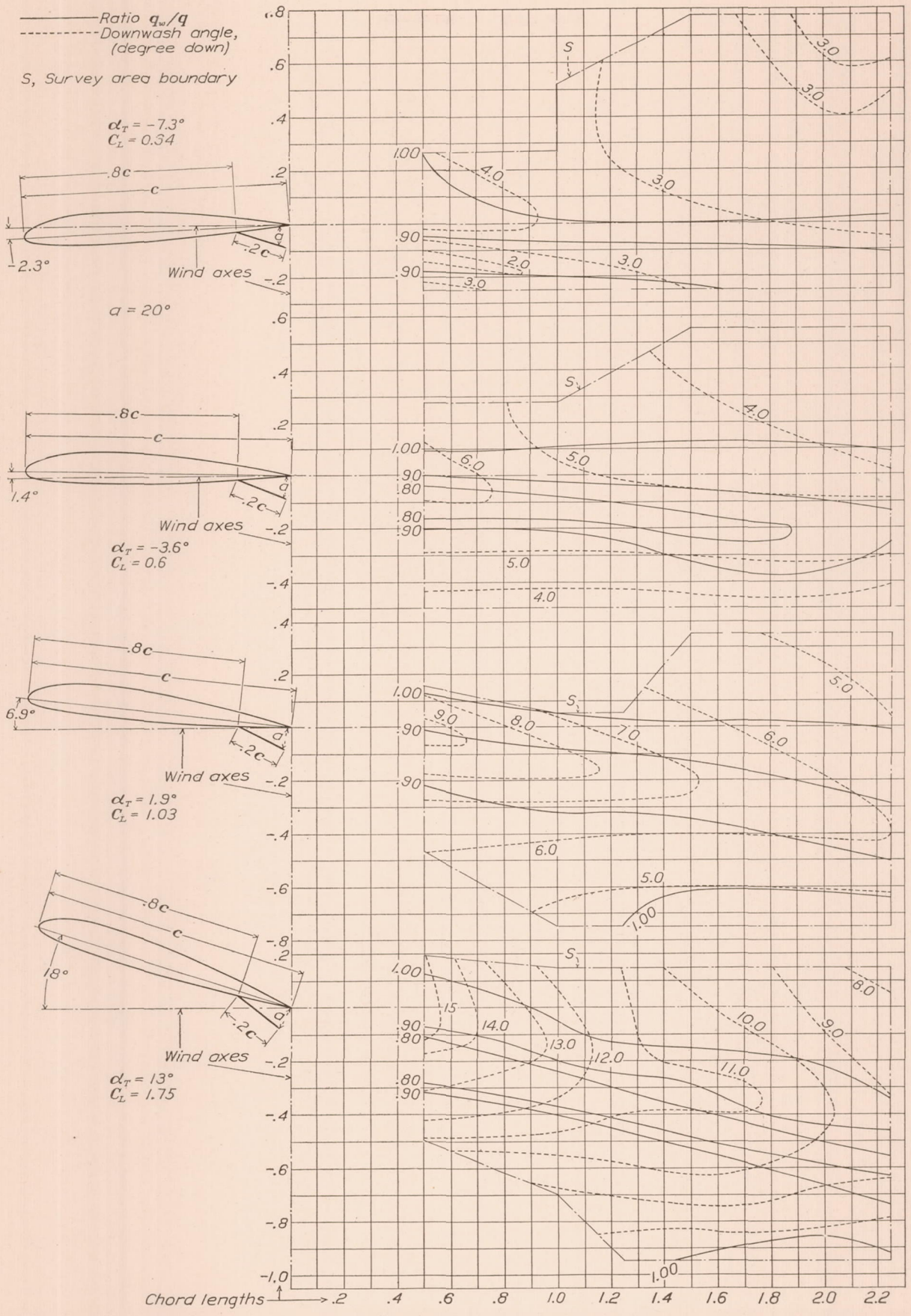

FIGURE 21.—Downwash contours for wing with 20 percent c flap hinged at 80 percent c, $\delta_F = 20°$.

NOTE.—δ_F is designated by a.

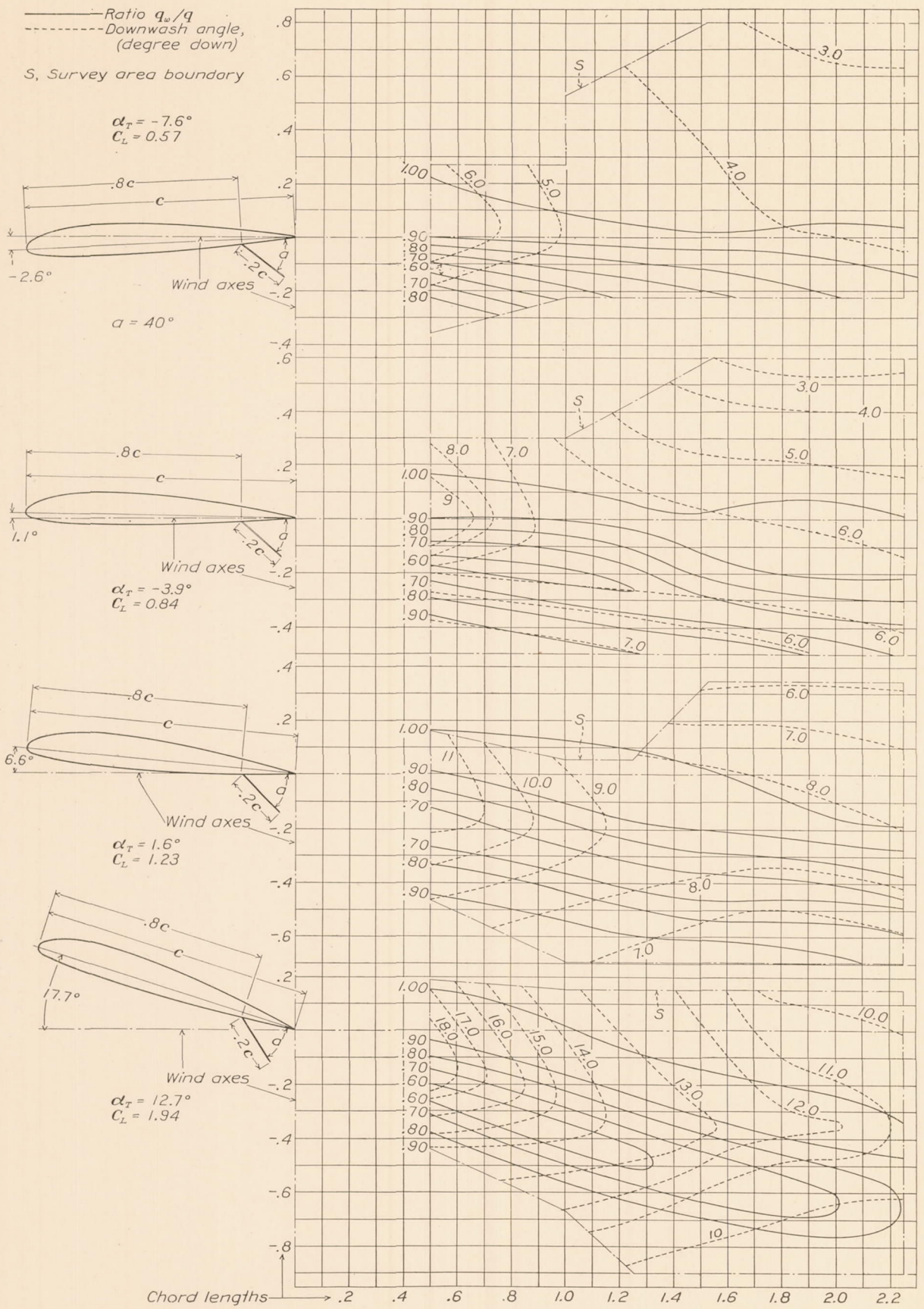

FIGURE 22.—Downwash contours for wing with 20 percent c flap hinged at 80 percent c, $\delta_F = 40°$.

NOTE.—δ_F is designated by a.

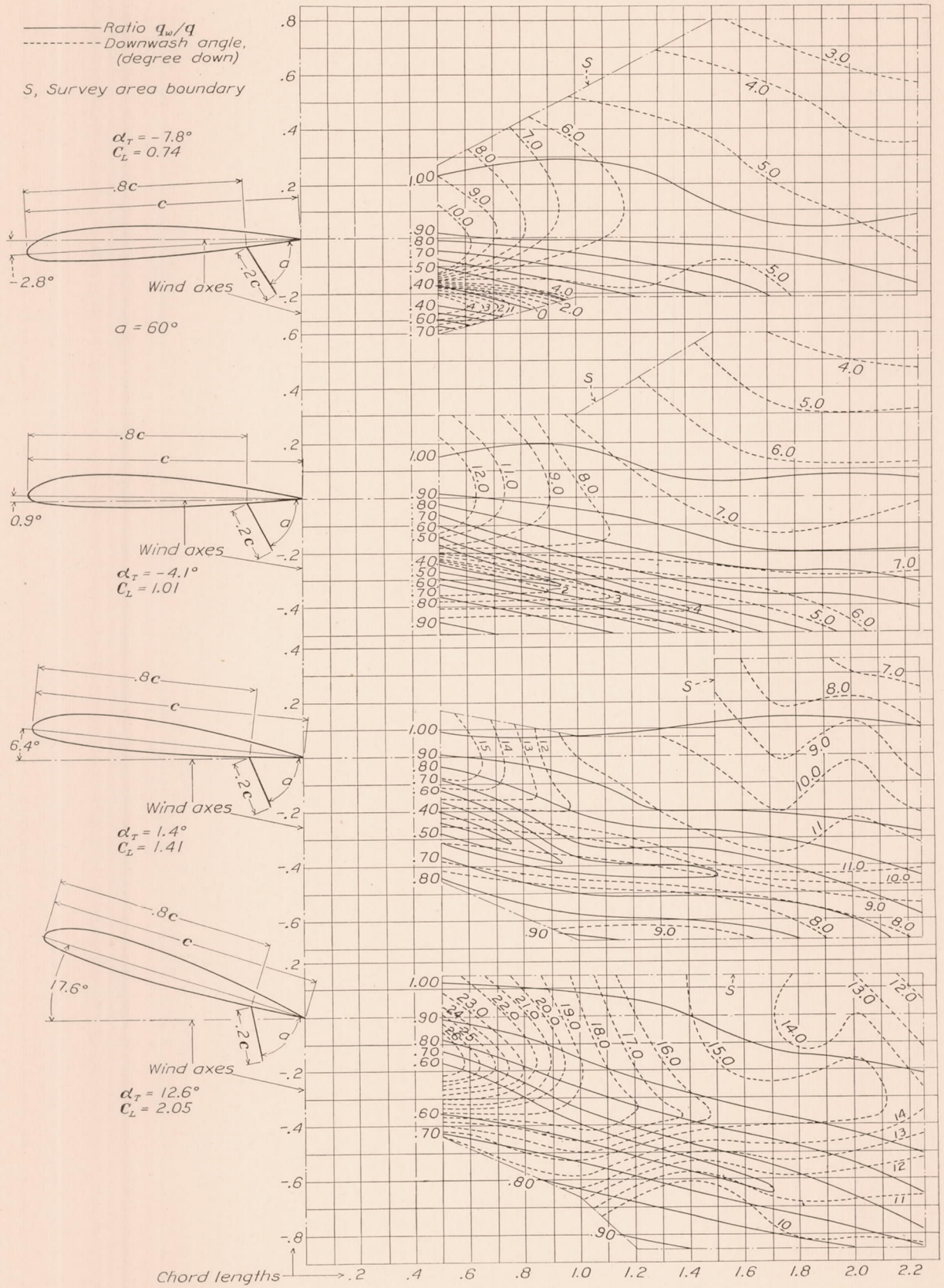

FIGURE 23.—Downwash contours for wing with 20 percent c flap hinged at 80 percent c, $\delta_F = 60°$.

NOTE.—δ_F is designated by a.

LOCATION OF TAIL PLANES

The downwash contours of figures 20 to 23 are of particular interest in indicating the effect of flaps on tail pitching moments. As the variations in downwash angles and the ratios of q_w/q with flap deflection differ throughout the wake, the effect of the flaps would depend upon the location of the tail surfaces with respect to the wing. The contours indicate that, at high angles of attack, tail surfaces located above the extended chord line of the wing would be subject to a greater increase in downwash with increase in flap deflection than would those below and would therefore be more effective in balancing the increased diving moment of the wing with the flaps down. This indication is in agreement with the fact that various low-wing monoplanes tested in the N. A. C. A. full-scale wind tunnel have shown less change in pitching moment with flap deflection than did the parasol Fairchild 22 when tested with the horizontal tail surfaces in place (reference 5). The higher tail locations are also more favorable in that there is less tendency for the tail surfaces to be carried into the low-velocity region of the wake at high angles of attack.

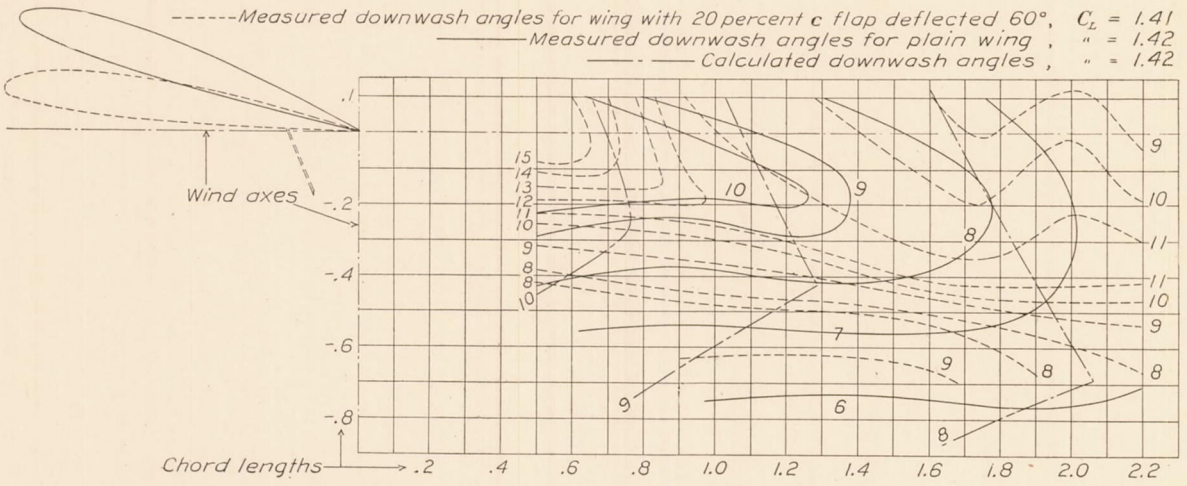

FIGURE 24.—Comparative contours of measured and calculated downwash angles.

CONCLUSIONS

The following conclusions are drawn from the results of this investigation of split trailing-edge flaps on a Fairchild 22 airplane.

1. The lift of the airplane increased with increase in flap chord and with increase in distance of the hinge axis from the leading edge of the wing.

2. For an increase in lift resulting from increase in flap chord the L/D ratio decreased, but for an increase resulting from movement of the hinge axis the L/D ratio remained practically constant.

3. Wing diving moment increased with increase in flap chord and with increase in distance of the hinge axis from the leading edge of the wing.

4. Flap normal-force coefficients were primarily a function of flap deflection and were dependent to a small degree upon flap chord, hinge-axis location, and the airplane attitude.

5. Flap center-of-pressure locations in terms of percentage flap chord from the hinge axis were independent of flap chord, hinge-axis location, and airplane attitude and varied only slightly with flap deflection.

6. Flap hinge moments varied with a power of flap chord greater than the square.

7. Split trailing-edge flaps materially affected the magnitude and distribution of pressures over the entire wing profile. At low angles of attack the predominant effect of the flaps was to increase positively the lower-surface pressures; at high angles of attack, to increase negatively the upper-surface pressures.

8. Existing empirical equations for computing downwash angles do not accurately define the pattern of downwash angles in the wake.

9. Air-flow surveys indicated that horizontal tail planes located above the extended chord line of the wing would be more effective than those below in counteracting the increased diving moment of the airplane with the flaps deflected.

LANGLEY MEMORIAL AERONAUTICAL LABORATORY,
NATIONAL ADVISORY COMMITTEE FOR AERONAUTICS,
LANGLEY FIELD, VA., *May 10, 1935.*

REFERENCES

1. Weick, Fred E., and Harris, Thomas A.: The Aerodynamic Characteristics of a Model Wing Having a Split Flap Deflected Downward and Moved to the Rear. T. N. No. 422, N. A. C. A., 1932.
2. Wenzinger, Carl J.: The Effect of Partial-Span Split Flaps on the Aerodynamic Characteristics of a Clark Y Wing. T. N. No. 472, N. A. C. A., 1933.
3. Wenzinger, Carl J.: The Effects of Full-Span and Partial-Span Split Flaps on the Aerodynamic Characteristics of a Tapered Wing. T. N. No. 505, N. A. C. A., 1934.
4. Joyce, Temple N.: Zap Flaps and Ailerons. Trans. A. S. M. E., vol. 56, no. 4, April 1934, pp. 193–201.
5. Wallace, Rudolf N.: The Effect of Split Trailing-Edge Wing Flaps on the Aerodynamic Characteristics of a Parasol Monoplane. T. N. No. 475, N. A. C. A., 1933.
6. Wenzinger, Carl J.: Wind-Tunnel Measurements of Air Loads on Split Flaps. T. N. No. 498, N. A. C. A., 1934.
7. Rhode, Richard V.: The Pressure Distribution over the Wings and Tail Surfaces of a PW–9 Pursuit Airplane in Flight. T. R. No. 364, N. A. C. A., 1930.
8. Parsons, John F.: Full-Scale Force and Pressure-Distribution Tests on a Tapered U. S. A. 45 Airfoil. T. N. No. 521, N. A. C. A., 1935.
9. DeFrance, Smith J.: The N. A. C. A. Full-Scale Wind Tunnel. T. R. No. 459, N. A. C. A., 1933.

TABLE I

CHARACTERISTICS OF THE FAIRCHILD 22 AIRPLANE AND SPECIAL WING

Weight (including 140 lb. in rear cockpit and 15 gal. gasoline)	1,467 lb.
Airfoil section	N. A. C. A. 2212.
Wing area, including ailerons	171 sq. ft.
Stabilizer area	15.8 sq. ft.
Elevator area	10.4 sq. ft.
Fin area	4.1 sq. ft.
Rudder area	6.0 sq. ft.
Wing span	32 ft. 10 in.
Wing chord	5 ft. 6 in.
Angle of wing setting	5.0°.
Dihedral	0.7°.
Distance back from leading edge to *c. g.*	1 ft. 6⅛ in.
Distance below thrust axis to *c. g.*	⅝ in.
Distance from *c. g.* to elevator hinge	13 ft. 2¾ in.
Flap span (total)	27 ft. 1 in.
Flap chord, 10 percent	6.6 in.
Flap chord, 20 percent	1 ft. 1.2 in.
Flap chord, 30 percent	1 ft. 7.8 in.
Flap area (total), 10 percent	14.26 sq. ft.
Flap area (total), 20 percent	29.14 sq. ft.
Flap area (total), 30 percent	44.0 sq. ft.

TABLE II.—VALUES OF p/q FOR WING AND FLAP

δ_F (degrees)	CN_w	α_T (degrees)	Surface	Wing station from L. E., percent wing chord											Flap station from hinge axis, percent flap chord				
				1	3	6	12	20	35	55	75	85	90	95	0	20	40	60	80
PLAIN WING																			
	−0.303	−10.9	Upper	0.94	0.58	0.28	−0.05	−0.15	−0.17	−0.15	−0.10	−0.05	0.00	0.05					
			Lower	−1.95	−1.55	−1.02	−.76	−.52	−.40	−.20	−.06	.00	.05	.06					
	−.027	−7.2	Upper	.60	.20	−.10	−.35	−.39	−.33	−.23	−.12	−.04	.00	.05					
			Lower	−.75	−.88	−.60	−.50	−.33	−.25	−.12	−.05	.02	.05	.08					
	.210	−3.5	Upper	.12	−.28	−.52	−.63	−.53	−.45	−.26	−.15	−.05	.00	.07					
			Lower	.00	−.23	−.24	−.22	−.16	−.13	−.05	.00	.05	.08	.14					
	.686	2.0	Upper	−1.58	−1.59	−1.52	−1.28	−.99	−.68	−.42	−.25	−.10	−.03	.04					
			Lower	.99	.58	.42	.26	.19	.04	.01	.03	.06	.12	.14					
	1.170	9.3	Upper	−4.37	−3.15	−2.62	−2.12	−1.42	−.90	−.50	−.20	−.09	−.02	.04					
			Lower	.68	.96	.81	.61	.46	.28	.15	.12	.15	.13	.08					
	1.399	13.1	Upper	−5.60	−4.15	−3.25	−2.45	−1.65	−1.00	−.54	−.21	−.06	−.01	.02					
			Lower	.28	.98	.91	.72	.58	.35	.23	.19	.18	.17	.12					
10 PERCENT c FLAP HINGED AT 80 PERCENT c																			
20	0.148	−7.4	Upper	0.61	0.10	−0.18	−0.39	−0.40	−0.39	−0.30	−0.20	−0.13	−0.10	−0.10	−0.22	−0.22	−0.22	−0.22	−0.21
			Lower	−.53	−.73	−.54	−.41	−.24	−.15	.01	.26	−.22	−.22	−.22	.34	.32	.23	.12	−.03
	.867	1.8	Upper	−1.65	−1.63	−1.53	−1.30	−1.04	−.74	−.48	−.30	−.24	−.20	−.15	−.25	−.25	−.25	−.25	−.25
			Lower	.95	.65	.45	.27	.20	.12	.16	.37	−.25	−.25	−.24	.46	.40	.29	.16	.05
	1.460	9.1	Upper	−5.20	−3.62	−2.85	−2.15	−1.56	−1.03	−.64	−.40	−.28	−.22	−.16	−.12	−.12	−.12	−.12	−.12
			Lower	.50	.96	.87	.67	.51	.36	.30	.46	−.10	−.10	−.10	.54	.50	.40	.27	.13
40	.313	−7.6	Upper	.45	.00	−.27	−.49	−.49	−.46	−.36	−.30	−.26	−.25	−.25	−.40	−.40	−.40	−.40	−.38
			Lower	−.37	−.56	−.44	−.29	−.18	−.08	.13	.41	−.39	−.39	−.39	.50	.48	.46	.35	.17
	1.003	1.6	Upper	−1.76	−1.70	−1.60	−1.38	−1.10	−.81	−.55	−.42	−.34	−.32	−.29	−.41	−.41	−.41	−.41	−.41
			Lower	.98	.70	.50	.32	.26	.20	.29	.55	−.43	−.43	−.43	.65	.64	.56	.40	.20
	1.595	9.0	Upper	−5.50	−3.68	−2.93	−2.25	−1.62	−1.07	−.70	−.46	−.36	−.32	−.29	−.35	−.35	−.35	−.35	−.33
			Lower	.46	.97	.91	.74	.61	.46	.45	.65	−.35	−.35	−.35	.79	.74	.65	.48	.26
60	.420	−7.7	Upper	.40	.00	−.27	−.51	−.55	−.50	−.40	−.37	−.34	−.32	−.31	−.41	−.41	−.41	−.41	−.39
			Lower	−.20	−.43	−.35	−.23	−.09	.03	.28	.48	−.45	−.45	−.45	.53	.52	.54	.53	.43
	1.125	1.5	Upper	−2.12	−2.00	−1.77	−1.50	−1.15	−.84	−.61	−.50	−.43	−.40	−.40	−.52	−.52	−.52	−.52	−.48
			Lower	.95	.75	.58	.38	.28	.27	.38	.60	−.51	−.51	−.50	.67	.65	.63	.60	.45
	1.680	8.9	Upper	−5.56	−4.00	−3.12	−2.36	−1.71	−1.12	−.75	−.53	−.45	−.40	−.38	−.41	−.41	−.41	−.41	−.41
			Lower	.25	1.00	.93	.71	.59	.45	.45	.66	−.43	−.42	−.43	.79	.78	.78	.65	.50
75	1.170	1.4	Upper	−2.37	−2.12	−1.86	−1.55	−1.20	−.86	−.61	−.50	−.43	−.40	−.38	−.52	−.52	−.51	−.51	−.50
			Lower	.95	.79	.62	.45	.35	.33	.47	.65	−.52	−.53	−.50	.70	.60	.56	.56	.41
20 PERCENT c FLAP HINGED AT 68 PERCENT c																			
20	0.241	−7.5	Upper	0.55	0.08	−0.20	−0.44	−0.46	−0.43	−0.34	−0.30	−0.25	−0.23	−0.20	−0.28	−0.28	−0.28	−0.28	−0.28
			Lower	−.50	−.65	−.44	−.31	−.20	−.08	.15	−.30	−.30	−.30	−.30	.38	.31	.20	.06	−.06
	.983	−1.7	Upper	−1.87	−1.80	−1.65	−1.39	−1.12	−.79	−.52	−.36	−.29	−.26	−.24	−.33	−.33	−.33	−.33	−.33
			Lower	.96	.72	.54	.35	.29	.23	.31	−.31	−.31	−.31	−.31	.52	.42	.26	.12	−.05
	1.453	9.0	Upper	−5.00	−3.45	−2.85	−2.23	−1.60	−1.05	−.67	−.45	−.34	−.29	−.25	−.25	−.25	−.25	−.25	−.25
			Lower	.60	.99	.85	.68	.51	.40	.40	−.24	−.24	−.24	−.25	.59	.49	.34	.20	.08
40	.554	−7.8	Upper	.25	−.18	−.46	−.64	−.60	−.53	−.46	−.40	−.39	−.36	−.35	−.43	−.43	−.43	−.43	−.43
			Lower	−.02	−.25	−.13	−.09	−.01	.15	.45	−.47	−.47	−.48	−.48	.59	.60	.54	.35	.14
	1.249	1.4	Upper	−2.52	−2.25	−1.93	−1.61	−1.28	−.93	−.65	−.50	−.46	−.43	−.42	−.52	−.52	−.52	−.52	−.52
			Lower	.99	.85	.66	.52	.43	.39	.56	−.55	−.55	−.55	−.55	.80	.72	.56	.37	.15
	1.741	8.8	Upper	−5.60	−4.28	−3.44	−2.53	−1.81	−1.20	−.79	−.56	−.49	−.42	−.41	−.49	−.49	−.48	−.48	−.47
			Lower	.35	.96	.94	.78	.66	.55	.61	−.48	−.48	−.48	−.48	.85	.75	.60	.44	.23

TABLE II.—VALUES OF p/q FOR WING AND FLAP—Continued

δ_F (degrees)	C_{N_w}	α_T (degrees)	Surface	Wing station from L. E., percent wing chord											Flap station from hinge axis, percent flap chord				
				1	3	6	12	20	35	55	75	85	90	95	0	20	40	60	80
20 PERCENT c FLAP HINGED AT 68 PERCENT c—Continued																			
60	0.734	−8.0	Upper	−.07	−.45	−.66	−.76	−.73	−.62	−.51	−.46	−.44	−.45	−.44	−.55	−.55	−.55	−.55	−.55
			Lower	.32	.06	.07	.11	.18	.31	.64	−.55	−.56	−.57	−.57	.63	.60	.75	.60	.37
	1.335	1.2	Upper	−2.95	−2.53	−2.11	−1.70	−1.39	−1.04	−.78	−.61	−.54	−.51	−.49	−.55	−.55	−.55	−.54	−.53
			Lower	.97	.90	.73	.56	.50	.52	.72	−.54	−.54	−.53	−.54	.80	.82	.75	.58	.35
	1.884	8.7	Upper	−6.50	−4.50	−3.60	−2.70	−1.96	−1.32	−.90	−.65	−.55	−.54	−.53	−.55	−.55	−.55	−.55	−.55
			Lower	.20	.95	.99	.84	.71	.67	.76	−.58	−.60	−.60	−.60	.88	.89	.81	.66	.46
20 PERCENT c FLAP HINGED AT 80 PERCENT c																			
20	0.053	−11.3	Upper	0.80	0.46	0.15	−0.18	−0.26	−0.31	−0.25	−0.25	−0.25	−0.25	−0.23	−0.35	−0.35	−0.35	−0.35	−0.35
			Lower	−1.40	−1.28	−.85	−.59	−.40	−.23	.00	.37	−.35	−.36	−.36	.43	.34	.22	.08	−.06
	.360	−7.6	Upper	.35	−.07	−.35	−.54	−.52	−.47	−.36	−.30	−.25	−.24	−.22	−.36	−.36	−.36	−.36	−.36
			Lower	−.27	−.52	−.40	−.30	−.20	−.09	.10	.35	−.36	−.36	−.36	.45	.36	.24	.10	−.01
	.619	−3.9	Upper	−.24	−.55	−.77	−.84	−.75	−.61	−.46	−.34	−.30	−.28	−.27	−.38	−.38	−.38	−.38	−.38
			Lower	.40	.00	−.05	−.09	−.05	.00	.15	.47	−.37	−.37	−.37	.52	.43	.29	.14	−.01
	1.054	1.6	Upper	−1.90	−1.85	−1.72	−1.47	−1.16	−.79	−.56	−.42	−.35	−.31	−.28	−.35	−.35	−.35	−.35	−.33
			Lower	.99	.65	.50	.31	.26	.19	.21	.45	−.38	−.38	−.35	.55	.45	.33	.24	.05
	1.622	9.0	Upper	−5.50	−3.85	−3.15	−2.41	−1.69	−1.10	−.68	−.42	−.32	−.28	−.25	−.19	−.19	−.18	−.18	−.17
			Lower	.10	.97	.90	.73	.57	.44	.38	.53	−.20	−.20	−.20	.63	.52	.42	.29	.12
	1.802	12.7	Upper	−6.35	−4.75	−3.70	−2.75	−1.85	−1.15	−.74	−.45	−.35	−.30	−.25	−.17	−.16	−.16	−.16	−.16
			Lower	.00	.99	.95	.85	.68	.50	.45	.61	−.18	−.19	−.19	.66	.55	.41	.30	.18
40	.298	−11.6	Upper	.77	.35	.06	−.24	−.34	−.36	−.34	−.34	−.34	−.34	−.33	−.50	−.50	−.50	−.50	−.50
			Lower	−1.06	−1.00	−.60	−.42	−.24	−.06	.24	.50	−.50	−.50	−.50	.52	.56	.54	.36	.10
	.613	−7.9	Upper	.20	−.15	−.41	−.61	−.60	−.50	−.43	−.40	−.40	−.40	−.40	−.55	−.54	−.54	−.54	−.54
			Lower	.10	−.28	−.20	−.09	−.02	.10	.27	.54	−.56	−.56	−.56	.62	.64	.53	.35	.10
	.929	−4.2	Upper	−.75	−1.00	−1.08	−1.06	−.89	−.70	−.52	−.47	−.44	−.42	−.42	−.58	−.58	−.57	−.57	−.57
			Lower	.63	.31	.21	.13	.12	.16	.34	.60	−.58	−.58	−.58	.70	.69	.55	.36	.13
	1.350	1.3	Upper	−2.55	−2.28	−2.00	−1.65	−1.28	−.92	−.70	−.57	−.51	−.50	−.49	−.56	−.56	−.56	−.56	−.58
			Lower	.98	.79	.62	.45	.36	.31	.36	.63	−.59	−.59	−.58	.78	.69	.56	.36	.11
	1.882	8.6	Upper	−5.60	−4.23	−3.38	−2.59	−1.80	−1.20	−.79	−.60	−.52	−.49	−.48	−.54	−.54	−.54	−.54	−.50
			Lower	−.20	.99	.93	.76	.63	.51	.50	.71	−.55	−.55	−.55	.85	.76	.61	.43	.20
	2.078	12.4	Upper	−7.00	−5.30	−4.05	−3.05	−2.05	−1.33	−.88	−.64	−.55	−.50	−.48	−.50	−.50	−.49	−.49	−.47
			Lower	−.40	.75	.98	.88	.73	.59	.53	.75	−.50	−.50	−.50	.90	.77	.65	.45	.23
60	.451	−11.8	Upper	.65	.21	−.06	−.34	−.40	−.41	−.40	−.42	−.42	−.42	−.42	−.56	−.56	−.56	−.56	−.56
			Lower	−.73	−.66	−.40	−.25	−.08	.10	.45	.49	−.57	−.57	−.56	.49	.55	.70	.70	.43
	.749	−8.1	Upper	.00	−.30	−.55	−.66	−.66	−.60	−.50	−.48	−.46	−.45	−.45	−.60	−.60	−.60	−.60	−.60
			Lower	.30	−.04	−.05	−.05	.09	.21	.50	.60	−.60	−.60	−.60	.64	.68	.77	.67	.37
	1.045	−4.4	Upper	−.86	−1.06	−1.14	−1.09	−.90	−.73	−.57	−.53	−.50	−.50	−.50	−.60	−.60	−.60	−.61	−.61
			Lower	.75	.46	.34	.25	.24	.30	.50	.68	−.60	−.60	−.60	.74	.76	.77	.64	.36
	1.471	1.1	Upper	−2.80	−2.44	−2.10	−1.70	−1.35	−1.00	−.75	−.67	−.62	−.59	−.56	−.68	−.65	−.64	−.64	−.63
			Lower	.99	.88	.72	.51	.45	.42	.58	.70	−.70	−.70	−.65	.96	.89	.80	.65	.36
	1.972	8.5	Upper	−6.60	−4.45	−3.52	−2.72	−1.95	−1.28	−.90	−.70	−.63	−.60	−.60	−.66	−.66	−.66	−.65	−.63
			Lower	.10	.99	.93	.81	.70	.60	.62	.80	−.65	−.65	−.65	.92	.86	.80	.65	.35
	2.198	12.3	Upper	−7.50	−5.50	−4.40	−3.15	−2.20	−1.45	−.96	−.71	−.65	−.64	−.62	−.56	−.56	−.56	−.56	−.56
			Lower	−.90	.70	1.00	.90	.79	.65	.65	.82	−.56	−.58	−.59	.93	.90	.81	.64	.38
20 PERCENT c FLAP HINGED AT 88.8 PERCENT c																			
20	0.339	−7.6	Upper	0.50	0.04	−0.25	−0.45	−0.45	−0.40	−0.32	−0.30	−0.22	−0.20	−0.19	−0.25	−0.25	−0.25	−0.25	−0.25
			Lower	−.55	−.64	−.46	−.34	−.22	−.12	.05	.26	.39	−.25	−.25	.44	.35	.26	.15	.05
	1.136	1.5	Upper	−2.00	−1.95	−1.73	−1.40	−1.11	−.79	−.54	−.39	−.33	−.29	−.25	−.24	−.23	−.22	−.21	−.20
			Lower	1.00	.73	.53	.39	.28	.22	.22	.36	.50	−.25	−.25	.55	.46	.35	.23	.10
	1.652	8.8	Upper	−5.00	−3.72	−3.04	−2.30	−1.62	−1.08	−.69	−.43	−.33	−.28	−.24	−.13	−.13	−.13	−.13	−.14
			Lower	.40	.99	.93	.75	.57	.43	.39	.49	.58	−.13	−.15	.63	.52	.40	.30	.16
40	.669	−8.0	Upper	.25	−.20	−.45	−.63	−.60	−.55	−.47	−.43	−.41	−.40	−.42	−.56	−.55	−.55	−.55	−.54
			Lower	−.05	−.34	−.24	−.16	−.07	.03	.22	.45	.55	−.59	−.60	.61	.61	.53	.37	.15
	1.395	1.2	Upper	−2.41	−2.10	−1.87	−1.53	−1.23	−.90	−.68	−.57	−.53	−.52	−.50	−.60	−.60	−.60	−.60	−.58
			Lower	.98	.81	.62	.44	.36	.30	.35	.53	.63	−.60	−.60	.70	.68	.58	.40	.17
	1.955	8.5	Upper	−5.70	−4.03	−3.24	−2.52	−1.76	−1.21	−.83	−.60	−.50	−.49	−.46	−.45	−.46	−.47	−.48	−.48
			Lower	.40	1.00	.93	.75	.62	.52	.50	.61	.74	−.45	−.45	.80	.78	.66	.50	.28
60	.885	−8.1	Upper	−.11	−.50	−.66	−.80	−.72	−.62	−.52	−.50	−.49	−.49	−.50	−.65	−.65	−.65	−.65	−.65
			Lower	.40	.00	−.02	−.02	.06	.18	.38	.54	.60	−.65	−.65	.70	.63	.71	.64	.45
	1.606	1.0	Upper	−2.91	−2.48	−2.10	−1.80	−1.39	−1.04	−.75	−.66	−.61	−.62	−.62	−.75	−.75	−.75	−.75	−.75
			Lower	.94	.90	.70	.55	.45	.40	.48	.62	.71	−.75	−.75	.78	.83	.79	.61	.38
	2.100	8.4	Upper	−6.20	−4.60	−3.42	−2.64	−1.90	−1.30	−.92	−.70	−.62	−.60	−.58	−.68	−.63	−.63	−.63	−.60
			Lower	.40	1.00	.93	.80	.69	.58	.58	.66	.79	−.68	−.68	.85	.79	.79	.65	.43
30 PERCENT c FLAP HINGED AT 80 PERCENT c																			
10	2.180	−7.5	Upper	0.55	0.15	−0.15	−0.40	−0.45	−0.40	−0.30	−0.24	−0.20	−0.19	−0.16	−0.14	−0.14	−0.14	−0.14	−0.14
			Lower	−.65	−.75	−.55	−.40	−.28	−.16	.00	.21	−.13	−.13	−.13	.26	.20	.13	.08	.05
	.969	1.6	Upper	−1.85	−1.78	−1.64	−1.35	−1.03	−.74	−.50	−.34	−.26	−.22	−.16	−.11	−.11	−.11	−.11	−.11
			Lower	.91	.64	.43	.28	.19	.14	.16	.30	−.10	−.10	−.10	.35	.29	.21	.15	.08
	1.544	9.0	Upper	−5.30	−3.60	−2.90	−2.20	−1.58	−1.03	−.64	−.40	−.28	−.24	−.19	−.07	−.07	−.07	−.07	−.07
			Lower	.55	1.00	.90	.70	.53	.40	.34	.43	−.09	−.09	−.09	.46	.39	.30	.23	.15
20	4.340	−7.8	Upper	.50	.05	−.23	−.47	−.50	−.46	−.40	−.36	−.34	−.33	−.32	−.39	−.38	−.38	−.38	−.37
			Lower	−.45	−.55	−.43	−.29	−.18	−.06	.10	.36	−.40	−.40	−.40	.44	.33	.23	.10	−.02
	1.185	1.4	Upper	−1.75	−1.68	−1.56	−1.38	−1.06	−.80	−.58	−.46	−.40	−.37	−.35	−.36	−.36	−.36	−.36	−.36
			Lower	.90	.66	.48	.35	.27	.21	.26	.48	−.34	−.34	−.34	.58	.43	.30	.16	.08
	1.810	8.7	Upper	−5.70	−4.10	−3.25	−2.45	−1.75	−1.15	−.78	−.56	−.45	−.40	−.36	−.30	−.29	−.28	−.28	−.28
			Lower	.35	1.00	.91	.74	.59	.48	.42	.60	−.30	−.30	−.30	.66	.54	.40	.28	.17
40	.820	−8.2	Upper	.04	−.31	−.55	−.68	−.64	−.56	−.46	−.49	−.50	−.50	−.50	−.64	−.64	−.64	−.64	−.64
			Lower	.34	−.03	−.04	−.01	.06	.18	.40	.58	−.65	−.65	−.65	.62	.65	.55	.35	.07
	1.540	1.0	Upper	−2.70	−2.32	−1.99	−1.63	−1.25	−.93	−.70	−.61	−.58	−.54	−.53	−.64	−.64	−.64	−.64	−.64
			Lower	1.00	.88	.70	.54	.45	.42	.52	.70	−.63	−.63	−.62	.80	.75	.60	.41	.22
	2.137	8.4	Upper	−6.50	−4.55	−3.54	−2.60	−1.91	−1.31	−.91	−.69	−.62	−.60	−.60	−.58	−.58	−.57	−.56	−.55
			Lower	.30	.98	.99	.84	.71	.60	.61	.75	−.60	−.60	−.60	.85	.84	.70	.50	.30

U. S. GOVERNMENT PRINTING OFFICE: 1935

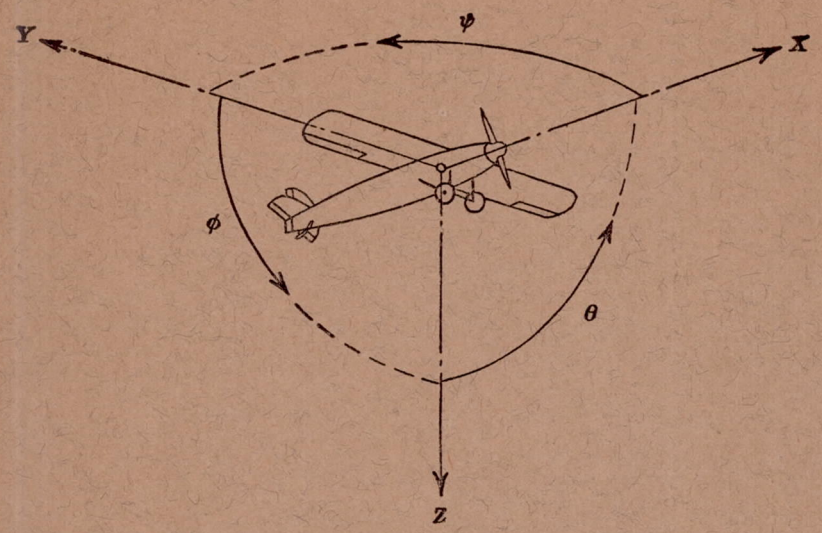

Positive directions of axes and angles (forces and moments) are shown by arrows

Axis		Force (parallel to axis) symbol	Moment about axis			Angle		Velocities	
Designation	Symbol		Designation	Symbol	Positive direction	Designation	Symbol	Linear (component along axis)	Angular
Longitudinal	X	X	Rolling	L	$Y \longrightarrow Z$	Roll	ϕ	u	p
Lateral	Y	Y	Pitching	M	$Z \longrightarrow X$	Pitch	θ	v	q
Normal	Z	Z	Yawing	N	$X \longrightarrow Y$	Yaw	ψ	w	r

Absolute coefficients of moment

$C_l = \frac{L}{qbS}$ (rolling) $\quad C_m = \frac{M}{qcS}$ (pitching) $\quad C_n = \frac{N}{qbS}$ (yawing)

Angle of set of control surface (relative to neutral position), δ. (Indicate surface by proper subscript.)

4. PROPELLER SYMBOLS

D, Diameter

p, Geometric pitch

p/D, Pitch ratio

V', Inflow velocity

V_s, Slipstream velocity

T, Thrust, absolute coefficient $C_T = \frac{T}{\rho n^2 D^4}$

Q, Torque, absolute coefficient $C_Q = \frac{Q}{\rho n^2 D^5}$

P, Power, absolute coefficient $C_P = \frac{P}{\rho n^3 D^5}$

C_s, Speed-power coefficient $= \sqrt[5]{\frac{\rho V^5}{P n^2}}$

η, Efficiency

n, Revolutions per second, r.p.s.

Φ, Effective helix angle $= \tan^{-1}\left(\frac{V}{2\pi r n}\right)$

5. NUMERICAL RELATIONS

1 hp. = 76.04 kg-m/s = 550 ft-lb./sec.
1 metric horsepower = 1.0132 hp.
1 m.p.h. = 0.4470 m.p.s.
1 m.p.s. = 2.2369 m.p.h

1 lb. = 0.4536 kg.
1 kg = 2.2046 lb.
1 mi. = 1,609.35 m = 5,280 ft.
1 m = 3.2808 ft.